Tool Design for and Process Optimization of an Automated Workstation for the Manufacture of Fiber Optic Gyroscopes

by

Wesley H. Williams

S.B., Mechanical Engineering, Massachusetts Institute of Technology, 1996

Submitted to the Department of Mechanical Engineering in
partial fulfillment of the requirement for the degree of

Master of Science in Mechanical Engineering

at the

MASSACHUSETTS INSTITUTE OF TECHNOLOGY

February 21, 1998

[June 1998]

Author.....
Mechanical Engineering
February 21, 1998

Certified by.....
Dr. Andre Sharon
Executive Officer, MIT Manufacturing Institute
Thesis Supervisor

Accepted by.....
Dr. Ain A.Sonin
Professor, Mechanical Engineering
Chairperson, Departmental Committee on Graduate Students

Tool Design for and Process Optimization of an Automated Workstation for the Manufacture of Fiber Optic Gyroscopes

by

Wesley H. Williams

Submitted to the Department of Mechanical Engineering on February 1, 1998, in partial fulfillment of the requirement for the degree of Master of Science

Abstract

Fiber optic gyroscopes are inertial navigation devices used in a variety of naval and aerospace applications, ranging from military applications to satellite launching and maneuvering, to commercial aviation. Optical gyroscopes consist of electrical and optical circuit components connected by optical fiber. The current process to assemble these gyroscopes is time-consuming and costly. It consists of a manual pigtailing of fiber leads onto components which are then manually spliced together. This splicing process consists of manually stripping the fiber of it acrylate coating, cleaning the bare glass portion of fiber, cleaving the ends of the fibers flat, fusion splicing the prepared fiber ends together, rejacketing the stripped portion remaining, and prooftesting the completed splice. The high degree of touch labor involved in this process results in inconsistent splice losses, long production lead times, and high production costs.

A machine has been designed, developed, and tested at MIT which automates the process of creating a fiber optic splice. The MIT machine moves a tray of optical components into position underneath fiber manipulators, and above a number of tools that work with these manipulators to perform each of the procedures in a splice. This research details the design of two splicing tools, (an automated fiber cleaver, and an automated rejacketer), as well as the fabrication of and process optimization of the entire optical assembly station. A number of significant fiber-optic handling issues such as non-destructive ways to tension fiber, and high viscosity fluid flow were addressed in the tool designs, and many process related issues were overcome during machine testing. The current Optical Assembly Station can perform repeatable, high quality splices at greatly reduced costs and times as compared to the manual process.

Thesis Supervisor: Dr. Andre Sharon
Title: Executive Officer, MIT Manufacturing Institute

Acknowledgments

In my experience as a student at MIT, I have had the privilege of working with some of the most competent and thought provoking scientists and engineers in the world. From these people I have learned much, and could not possibly have room for them all in this section. Of the names that will be mentioned however, the first must be my advisor, Dr. Andre Sharon. He has either directly or indirectly influenced every aspect of my research, and has shown me a practical side to machine design that I could never have gotten from a textbook. Much thanks should also go to my lab partners, David Roberts and Wayne Hsiao. They put up with my inability to adhere to a schedule, and slapped me around as necessaryWayne was always there to point out the lack of beauty in my overly practical designs, and I would like to think that my future designs will reflect this criticism (in style Wayne, not cost). As well, Mr. Hsiao, as well as Brandon Gordon, helped me to develop a philosophy of beer-drinking that in no way contributed to the speediness of my Thesis writing. Fred Cote' and Gerry Wentworth helped much in the area of machining, and let me run a Bridgeport at times while sleeping. Gunter Neidermeyer must be thanked for his excellent coding toward the projects end, as well as for being a general know-it-all. Our machine could not have been completed without the expert assistance of Ron Lill, Chiang Liu, and Eric Meece of Vytran Corporation, who took the Newark shuttle countless times to watch me slave away in Building One. Finally, thanks goes to Marshall Nauck, Bill Schultzenberg, John Shannon, Matt McQuewen, and the rest of the group at Honeywell for paying my way through grad school, among other things. Matt gets special credits for showing me all of the really terrible bars in Phoenix.

Chapter 1

1. Introduction

This chapter introduces inertial navigation systems and how gyroscopes are used in these systems. It then compares two of the gyroscopes currently used. An introduction of fiber optic gyroscopes follows, that includes the theory behind them, as well as the components and fiber types used in a circuit. The overall project initiative is then discussed, as well as the generic Integrated Fiber Optic Gyroscope (IFOG) assembly, and the transition from manual to automated processes in these operations. Finally the research goals and outline of this thesis are listed.

1.1 Inertial Navigation Systems

Inertial navigation systems are devices used to measure acceleration in automobiles, ships, airplanes, guided missiles, rockets, and a number of other craft that need to be accurately guided from one place to another. Once an initial reference position is known, such a device can accurately perform its task. An inertial navigation system consists of three "rate gyroscopes," which essentially measure rotation rate, mounted on three orthogonal axes , yielding the total acceleration of the object that it is mounted to in three dimensional space. Most inertial navigation systems today fit within a volume the size of a shoe box or smaller, and are simply mounted to some structural component of the vessel for which navigation is being performed.

1.2 Rate Gyroscope Performance

The performance of an individual (single axis) gyroscope is measured with a quantity called its "angular rate error," or "drift." This is a measure of the number of degrees per hour the gyroscope yields when it is held fixed (no rotation about its principle axis) for a set period

of time. This is essentially how much error would be in the actual vs. measured position of a guided vessel in one hours time. Ideally this error would be zero, but due to imperfections in the components of the gyroscopes, every finished product has some drift. Obviously, the smaller the drift, the more precise and reliable the gyroscope, and gyroscopes are divided into categories on the basis of this measure. Tactical grade gyroscopes, used in such applications as torpedo guidance, remote controlled automobiles, and unmanned aircraft have drifts of < .05 degrees/hour. Navigation grade gyroscopes, used in commercial aviation and long-range tactical missiles, and precision grade gyroscopes, used in space applications and strategic ballistic missile guidance exhibit rate errors of < .01 degrees/hour.

1.3 Fiber Optic vs. Mechanical Rate Gyroscopes

There are currently two distinct classes of rate gyroscope in general use. These are "mechanical gyroscopes" and "optical gyroscopes." As the name implies, mechanical gyroscopes employ a mechanical gyroscopic effect (the torque induced by rotating a spinning mass off axis of its spinning) and consist of such a spinning mass and platform (gimbals, etc.) on which this mass resides. [Draper, p. 563]. In order to provide measurable results, mechanical gyroscopes are often quite large and heavy. Also, because the consist of actual moving parts, reliability and repeatability are very difficult to attain. For these reasons, optical gyroscopes have rapidly been replacing mechanical gyroscopes for the last twenty or so years. Optical gyroscopes use light rather than mechanical means to sense rotation. One type of Optical gyroscope that is gaining prominence is the fiber optic gyroscope. Fiber optic gyroscopes are much smaller and lighter than their mechanical counterparts, and, with no moving parts, exhibit fewer problems that can increase drift or render them inoperable. Coupled with increased reliability, the potential for better performance and lower production costs are driving the use of fiber optic gyroscopes in many of today's inertial navigation systems.

1.4 Fiber Optic Gyroscopes

1.4.1 Optical Fibers

Before a detailed discussion of Fiber Optic gyroscopes, a brief explanation of optical fibers in general is in order. Optical Fibers are manufactured in a number of forms for as many applications, ranging from communications to navigation. The type of fiber used in fiber optic gyroscopes is called "single mode" fiber, indication that it carries light of a limited frequency range. This fiber

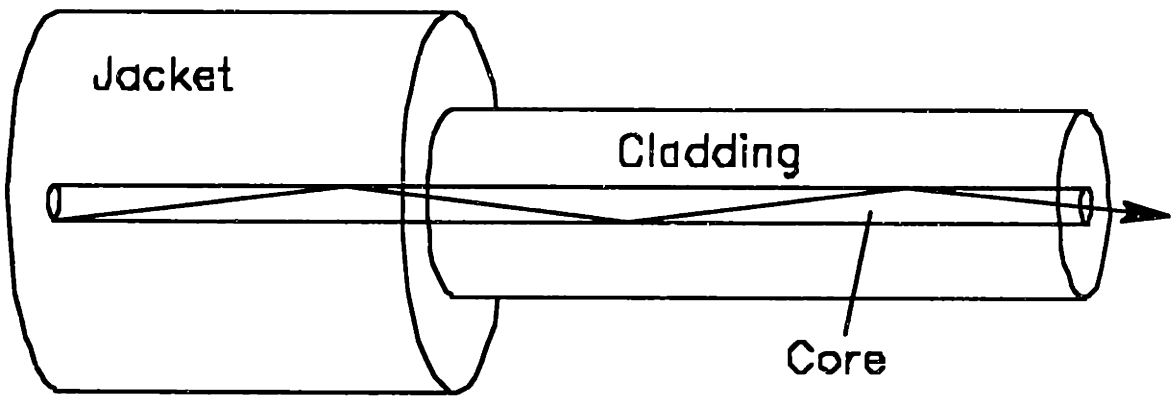

Figure 1.1: Light Propagation Through Optical Fiber

is composed of three distinct regions, as seen in Figure 1.1. The core and cladding are regions of glass with different refractive indices while the jacket is a protective outer layer of acrylic. A typical single mode fiber has a core diameter of < 10 μm, a cladding diameter between 80 and 130 μm, and an outer diameter, (including jacket) between 125 and 250 μm. In order for light to propagate down the core with minimal loss through the surrounding cladding, the index of refraction of the core must be higher than that of the cladding. Three types of single mode fiber are used in optical gyroscopes. The first of these is regular single mode (SM) fibers, which have circular cores on the order of 5 - 10

μm in diameter and allow all orientations of light to pass through. The second type, called polarization maintaining (PM) fibers , may have an elliptical core or stress rods that produce significant differences in the refractive indices between the minor and major axes of the ellipse. This results in rapid light propagation along one axis and slow light propagation along the other. In this way, optical power along the two axes can be differentiated. The third type of fiber used is Polarizing (PZ) fiber, which also has an elliptical core, but has an erbium doped cladding that allows only a certain wavelength of light to pass through the core.

1.4.2 The Sagnac Effect

A fiber optic gyroscope is able to measure the rate of rotation about a particular axis through utilization of the Sagnac Effect [Ezkial, p.15]. This effect is best described through a thought exercise. Imagine that a thin disc (say, the width of an optical fiber) is laying on the page, as shown in figure 1.2. Imagine that the disk has a length of optical fiber wrapped around it clockwise from point B to Point C, and that the fiber-disk unit is free to rotate about an axis passing through its center and perpendicular to the page, but for the present time is held stationary. If one light beam is sent clockwise from B to C at the same time as another light beam of equal phase is sent counter-clockwise from C to B, it is clear that the path length over which both beams have traveled is identical, and, furthermore, that if measured at their final positions both beams will still exhibit identical phase.

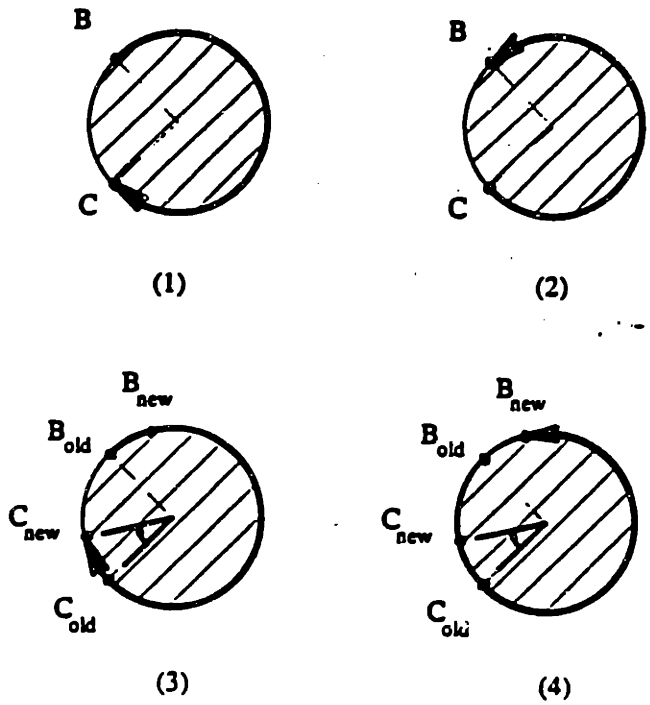

Figure 1.2: (1) Clockwise light path, no rotation
(2) Counterclockwise light path, no rotation
(3) Clockwise light path, clockwise rotation
(4) Counterclockwise light path, clockwise rotation

Now considering that the speed of light is constant through a given medium, imagine that immediately after the two counter propagating beams are released from B and C, the disc starts rotating clockwise at a rate Ω (see Figure 1.2-(3) and 1.2-(4)). Because of the rotation during the time that the beams are traveling around the perimeter of the disc, the path length that the clockwise propagating beam travels is longer than it was for the case of no rotation. The beam starts at the old location of B and ends at the new location of C. Conversely, the path length of the counterclockwise propagating beam becomes shorter than the case for no rotation. The beam starts at the old position of C and ends at the new position of B. This difference in path length results in a phase difference between the two beams, and it follows that the rate of disc rotation can be determine from this phase difference. This is the Sagnac Effect.

In the previous discussion, the light beams are shown to propagate through less than one full circumference of the disc. In reality, this limited length for light propagation would result in an almost indistinguishable phase difference between the two beams. To enhance the measurement sensitivity of this phase difference, fiber optic gyroscopes utilize a core with many wrappings of optical fiber. Given a disk of area A, rotating at an angular rate Ω, and wrapped with N turns of optical fiber, the phase difference, $\Delta\Phi$, between counter propagating beams is:

$$\Delta\Phi = (8\Pi AN/\lambda c)\Omega$$

where λ and c are the wavelength of the light and the speed of light in a vacuum, respectively [Ezekial, p.14]. The acronym for the fiber optic Gyroscope is IFOG, which stands for Interferometric Fiber Optic Gyroscope.

1.4.3 Generic IFOG Circuit

The generic IFOG circuit for one axis consists connected to on another by optical fiber, as shown in Figure 1.3. These include a light source, a 1x2 coupler, an integrating optics chip (IOC), a coil of many wrappings of fiber, and a photodetector.

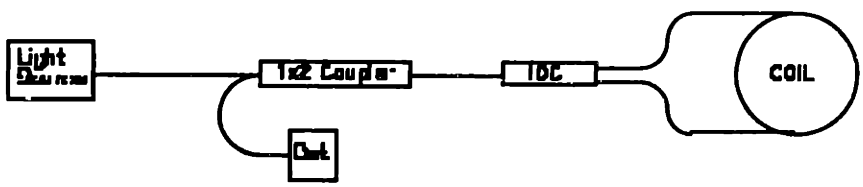

Figure 1.3: Layout of Generic IFOG Circuit

The light source emits light of a known wavelength into the fiber. This light passes through the 1x2 coupler and then through the IOC (which consists of a polarizer, modulator, and 50/50 beam splitter). This chip yields two identical output beams that then travel in opposite directions around the fiber coil. The polarizer helps to reduce the effects of noise in the circuit. The modulator increases the gyroscopes sensitivity at low rotation rates and also allows measurement of rotation direction (it does this by inducing a phase difference between the counter propagating beams) [Le Fever, pp. 125-127] [Ezekial, p.15]. Once through the coil, the counter propagating beams meet up again at the IOC, where they combine and interfere with each other. This resultant light beam then propagates back to the 1x2 coupler, where half of the beam is sent to the photodetector for a measurement of its light intensity and the other half is lost through the light source. As discussed above, a varying phase shift in the resultant beam varies the intensity measured at the photo detector. If the coil is not rotating, there is only the known phase shift induced by the modulator. The presence of coil rotation, however, generates an additional phase shift in the counter propagating beams due to the Sagnac Effect which results in a change in light intensity at the detector.

1.5 Inertial Measurement Unit (IMU)

As discussed previously, inertial navigation systems for use in air planes and missiles, for example, require monitoring of three rotation rates about orthogonal axes. Figure 1.4 shows an example of an inertial measurement unit containing three single-axis IFOG's. Each of the coils is mounted orthogonal to the other two. All other optical components are placed at various locations on this base structure and the optical fiber connecting the various components is carefully guided around and affixed to the structure itself.

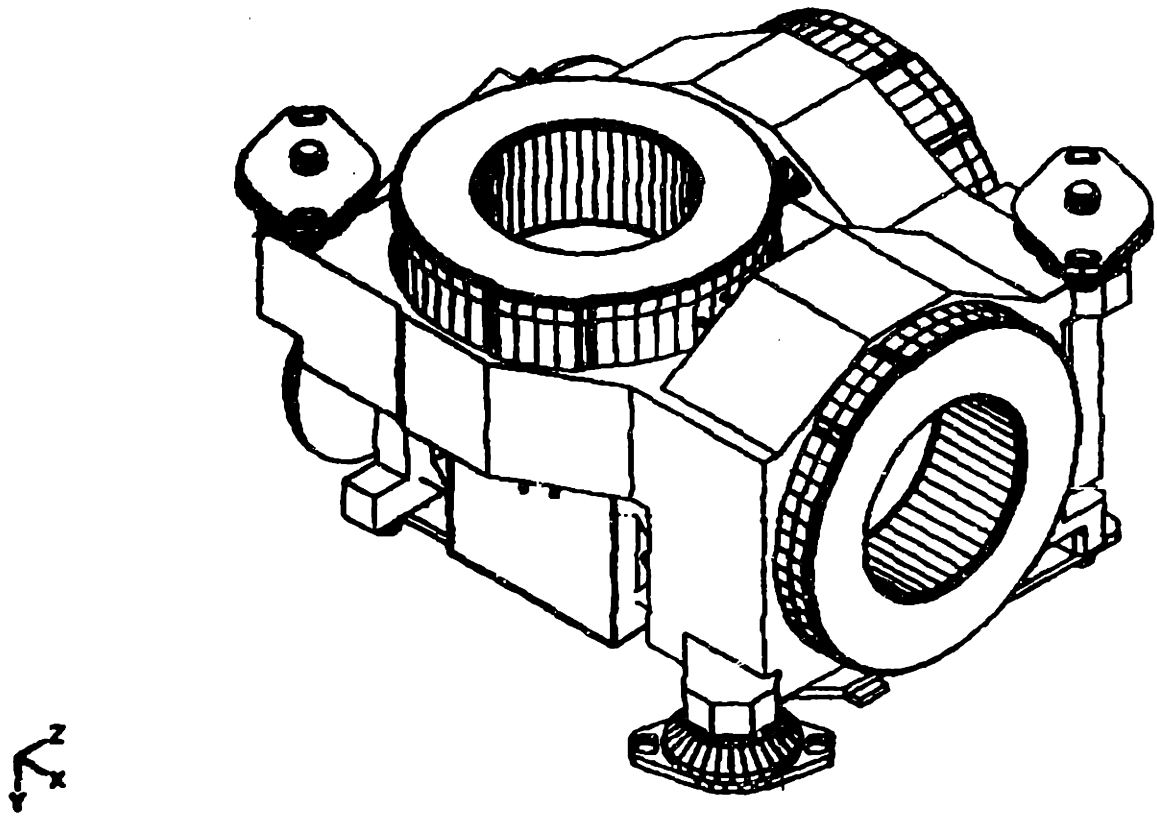

Figure 1.4: Inertial Measurement Unit

1.6 Project Initiative

The initiative of the MIT Manufacturing Institute has been to build an automated workstation capable of performing the splices in a number of IFOG circuits. This means that the station is able to accommodate at least four different fiber types, and many types of optical circuit components. The station receives a tray of optical components arranged in an organized manner with the fiber leads of each component oriented uniformly. The station then performs all of the necessary splice connections between all of the components, and the tray is removed to allow manual construction of the entire inertial measurement unit off line. The current method to complete this process entails a large amount of human touch labor, leading to large product lead times and low-repeatability process steps. The MIT automated assembly station, by divorcing a large amount of human labor and error from the process, will significantly lower the production time and raise process step repeatability.

1.7 Discussion of Generic IFOG circuit assembly

1.7.1 Splice Locations and fiber types IFOG circuit

Figure 1.5 shows the splice locations in a generic IFOG circuit. The lines emanating from each component represent optical fiber leads that are pigtailed to the components prior to the splicing procedure. The cross marks represent the areas where splices must be performed. The fiber types emanating from each component are generally different from one another. In order for an entire circuit to be successful, each splice in the circuit must be to specification. If four out of the five splices are good, but the fifth splice is faulty, then the performance of the entire circuit is compromised.

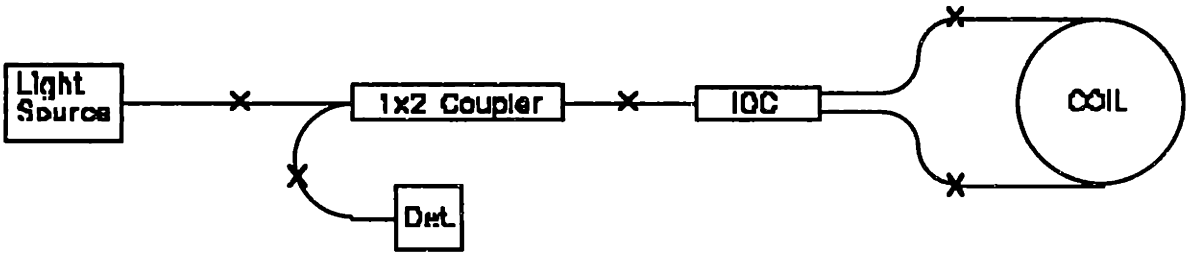

Figure 1.5: Splice Locations in an IFOG circuit

1.7.2 Splice Quality

A fiber optic splice consists of bringing two optical fiber ends to a molten state and then fusing them together. During this fusing, splice quality depends on two things. The first, and most important, is how well the cores of the respective fibers align, and, consequently, how continuos the light propagating portion of the splice is. An optically acceptable splice must exhibit less than some specified dB loss. Optical dB loss is a function of the light intensity (power) measured before a splice, and the light intensity measured after a splice:

$$dB_{loss} = -10\log(\text{powerin}/\text{powerout})$$

The second is the physical strength of the spliced area. If the fusing of the respective claddings is poor, or if any part of the splicing procedure compromises the claddings integrity, (i.e. cracks, contaminates) then this will result in a physical weakness in the spliced area. For this reason, the physical strength of a splice is tested by applying an amount of tension to the spliced area greater than any stresses expected during the lifetime of the component. This process is called "prooftesting."

1.7.3 Generic Splicing Steps and Motivation for Automation

The current manual fiber optic splicing process involves six steps. These steps, shown graphically in Figure 1.6, are detailed below:

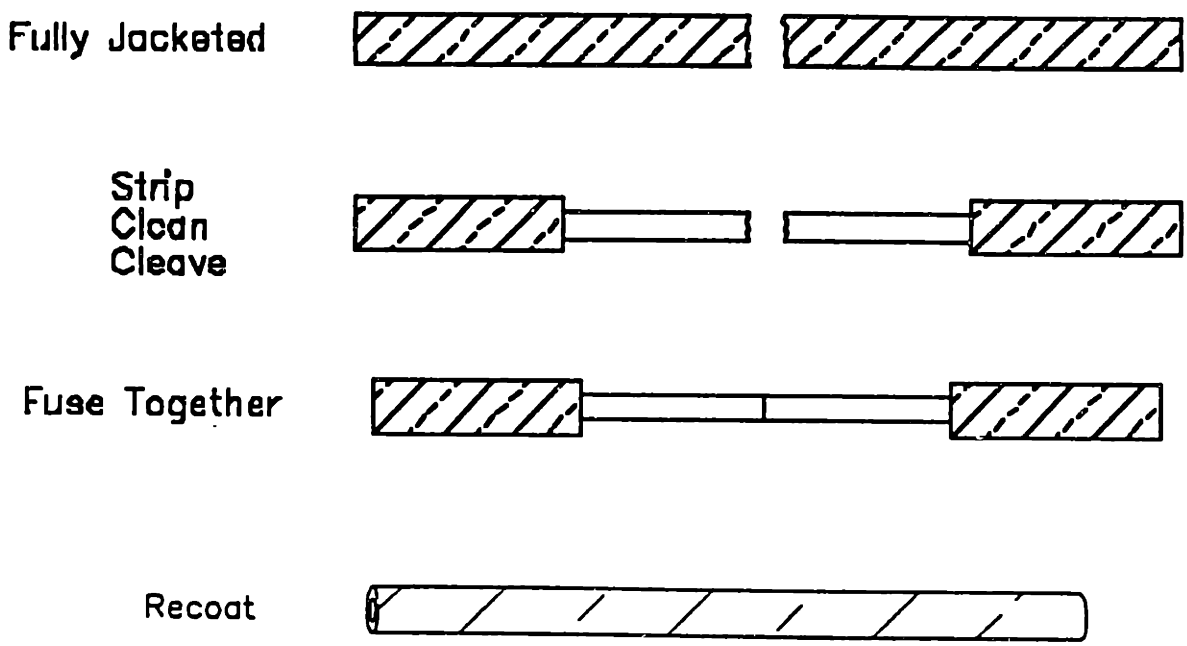

Figure 1.6: Steps Involved in Fiber Splicing

Step 1: Stripping: The fiber leads begin as fully jacketed and broken at some toleranced length. The first step is to remove the acrylic coating around the cladding, this is called stripping. In the manual process, this is performed with either a hand-held stripping tool or a razor blade. As these involve putting sharp metal objects in contact with the bare glass of the cladding, the operator has to be very careful not to damage this cladding during the strip.

Step 2: Cleaning: After most of the acrylate has been stripped from the fiber, there remains fine particles of it, as well as dirt left from the stripping tool. Also, some PM

fibers have a buffer of silicone between the jacket and the cladding, which is not removed during the strip. For these reasons, the next step in the splicing procedure is to clean off these particles to leave bare glass. The manual process for cleaning fibers entails wiping them with acetone dipped swabs, or some heavier solvent, such as methyl chloride to remove the silicone from PM fibers. As with stripping, this step involves much stress on the cladding, which can lead to micro cracks, and problems later in the process.

Step 3: Cleaving: After the fiber is stripped and cleaned, its endface is cleaved to be as smooth and flat as possible. This entails tensioning the fiber uniaxially and propagating a crack through it. If done properly, this results in a smooth, 90 degree endface. Most manual cleaving is done with very expensive hand held tools that require frequent maintenance in order to produce consistent cleaves.

Step 4: Fusing: Once the two fiber leads to be spliced have been stripped, cleaned and cleaved, the next step is to align and connect them. The alignment is done either by visual alignment and vision control, or by monitoring the light intensity passing through the splice location and maximizing this intensity. Once the alignment is complete, the fiber ends are melted by some local heating element and thereby fused together. This, the most important and delicate part of the entire process, is usually performed by partially automated fusion, or spark-gap splicers.

Step 5: Rejacketing: After the fibers are connected, and the actual splice is complete, the next step is to put a new coating of acrylate over the bare glass section remaining. The rejacketing material, usually an ultra-violet curable epoxy, is applied around the bare cladding and cured into place. This is usually done by placing the unjacketed portion into a fiber shaped mold, filling this mold with rejacketing material, and exposing the area to ultraviolet light. This is a manual process that requires much cleaning between rejackets.

Step 6: Prooftesting: The final step in a fiber splice is a prooftest of the type described in Section 1.6. Here the rejacketed area is subjected to a tensile stress test to ensure the integrity of the spliced area. As with each of the other steps in the current manual process, this step is performed in a separate station, with a significant amount of touch labor for each station. In fact, if one considers the assembly of an entire IFOG circuit that contains five separate splice locations, adding up the current process times and splice to splice movements yields a total assembly time of close to 5 hours. When compared to the 62 minute target time for the automated process , the impetus for the Optical Assembly Station becomes clear.

1.9 Research Goals and Outline of Thesis

The goal of this research was to design build and test an automated optical assembly station that has the ability to splice together trays of fiber lead optical components and meet the target process times. More specifically, this research details the design of two components of the workstation, as well as the assembly and testing of the entire station.

Chapter 2 begins with detailed designs of the portions of the station designed prior to the research in the thesis, and continues with the conceptual designs of the Automated cleaving and rejacketing tools. Chapters 3 and 4 give detailed designs of the Cleaver and Rejacketer, respectively. Chapter 5 details the research done to ensure the compatibility between the splicing tool and the rest of the workstation. Finally Chapter 6 discusses machine testing and process optimization, and concludes with recommendations for future work.

Chapter 2

2. Design of the Optical Assembly Station

This chapter begins with an overview of the detailed design of some of the major components and processes of the Optical Assembly Station which were complete at the onset of the research primary to this thesis. It then gives an outline of the conceptual autoated process of the Optical Assembly Station. It ends with the conceptual designs of the Cleaving Tool and Rejacketing Tool.

2.1 Optical Assembly Station Overview

2.1.1 Functional Requirements

There are three overall functional requirements for the OAS. They are as follows:

1. It must be able to perform all of the necessary steps in order to complete a fiber optic splice.
2. It must be able to accommodate a variety of optic circuits.
3. It must be able to perform active fiber alignment and measure the optical power loss at each splice.

As discussed in Chapter 1, the first functional requirement mandates that the OAS can strip, clean, and cleave fiber leads, fusion splice these leads, rejacket and then finally prooftest the splice to set standards. The second functional requirement mandates that the OAS has the capability to splice any optical circuit, not just those used in IFOG's. This required that the OAS be designed around accepting component trays that contain all of the components with their fiber leads arranged uniformly. These trays, which have a standardized interface with the OAS, are to be prepared and loaded by an operator, and then removed from the

station upon the completion of the circuit. An example of such a tray is shown in Figure 2.1. Although this particular tray contains the generic IFOG circuit discussed in Chapter 1, one can see that the components and splice locations could be moved to accommodate a variety of optical circuits. The OAS will act in the same manner with any tray, simply adjusting work locations to accommodate new trays.

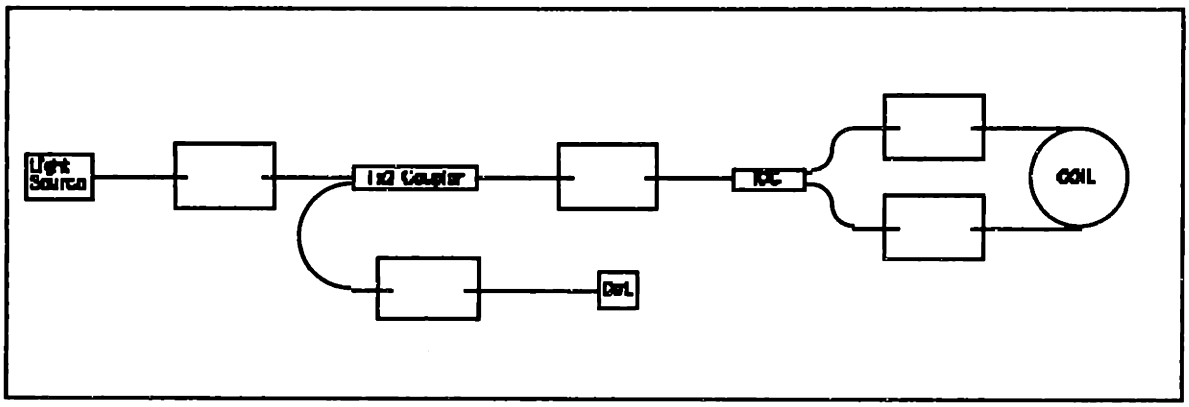

Figure 2.1: Single Axis Component Tray

The third functional requirement mandates that the OAS have the ability to measure the light passing through the splice location before, during, and after the splice is performed. This is accomplished by placing a photodetector one hole downstream in the circuit from the hole where the splice is occurring. In this manner the light throughput can be monitored during the splice, and compared with the light intensity before the splice. This is illustrated in Figure 2.2, where the holes are numbered in the order of the splicing operations, the dashed line surrounds the hole where the splice is occurring, and the circled "P" represents the photodetector. For the completion of this circuit, the photodetector would first be placed in hole 1, and the initial intensity from the light source would be measured. The photodetector would then be moved to hole two, while the leads in hole 1 are spliced together. In this way the light intensity can be measured throughout the splice, and the final, post-splice reading at hole 1 can be used to measure the loss, as well become the pre-

loss measurement for hole 2. This process is repeated until the circuit is complete. Of note is that the final component in this and many other optical circuits is itself a photodetector, so the final circuit loss can be measured.

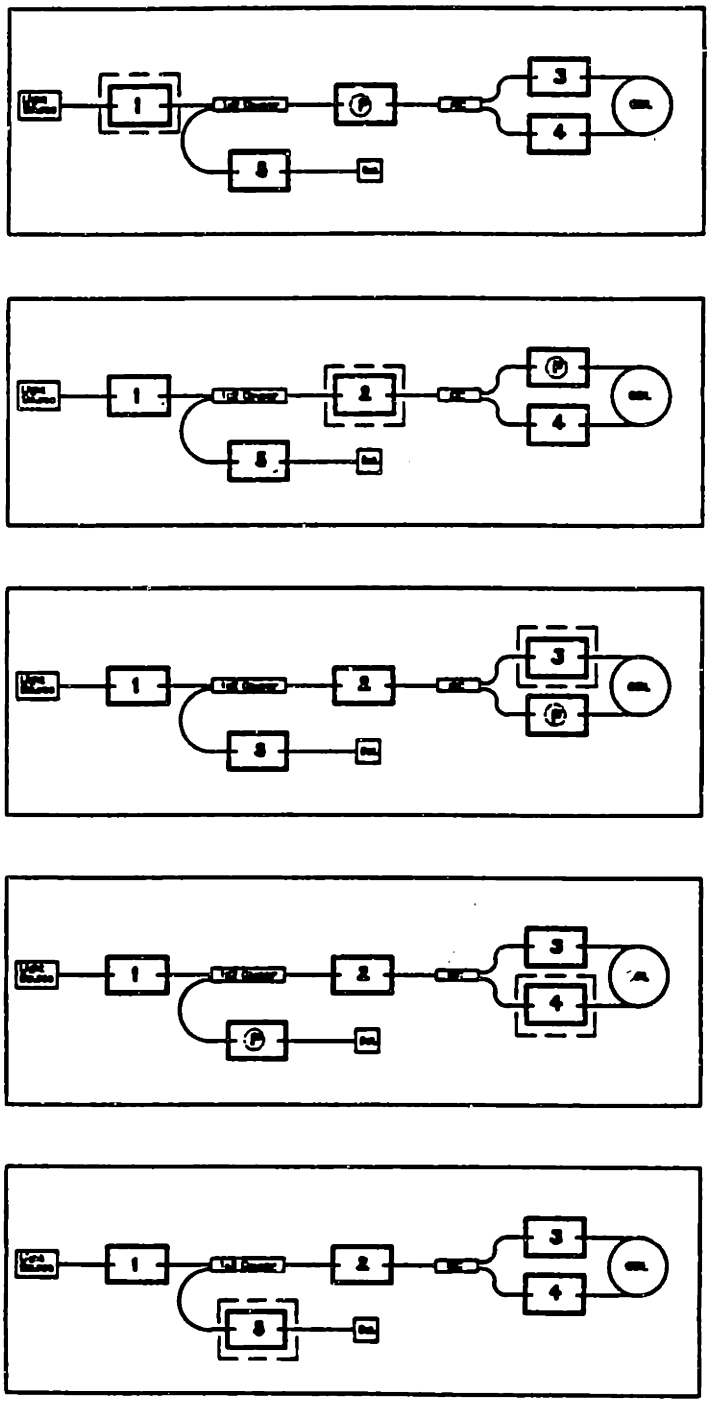

Figure 2.3: Photodetector Placement During OAS Operation

2.1.2 Station Architecture

Figure 2.3 shows a modular breakdown of the OAS. It consists of five modules: the Tray Manipulation Module, the Tool-Changing Module, the Photodetector Manipulation Module, the Fiber Manipulation Module, and the Toolbox Items.

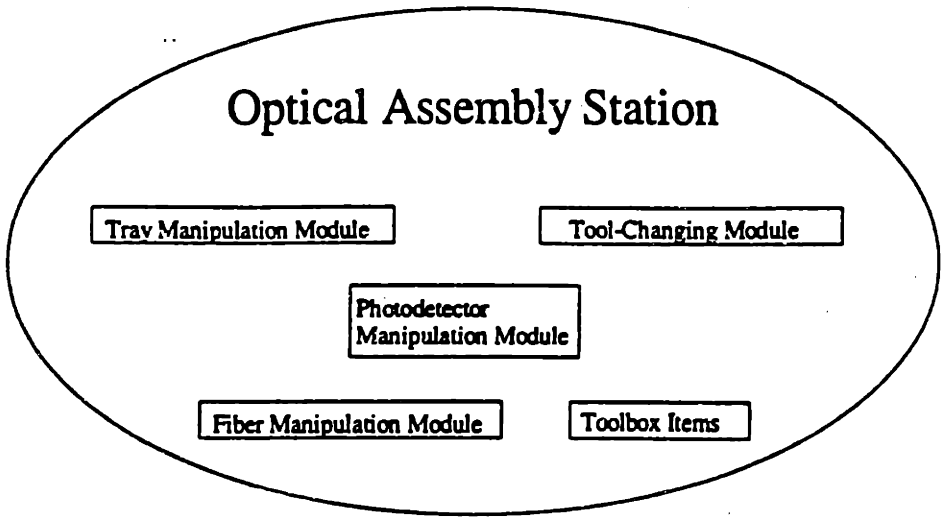

Figure 2.3: Modular Breakdown of the OAS

As envisioned the OAS works as follows: An operator loads a tray into the Tray Manipulation Module, which has the ability to move it to any position in a horizontal plane of a specified geometry. The Tray Manipulation Module moves the respective tray holes into position beneath the Fiber Manipulation Module, which consist of manipulators that can move both fiber leads with four degrees of freedom. The Fiber Manipulation Module is fixed in the Splicing Area, or fiber work location, where all the splices are actually performed. Underneath the Tray is the Tool Changing Module, which moves each of the toolbox items, and the Photodetector to the Splicing area, where these tools work, sometimes in conjunction with the Fiber Manipulation Module, to perform all of the operations in a splice and measure the light intensity as needed.

2.1.3 Breakdown of OAS Design Responsibility

The design and completion of the OAS has been a joint effort between MIT and the sponsor company. At the onset of the research in this thesis, the MIT Manufacturing Institute was completing the design of the Tray Manipulation Module, the Fiber Manipulation Module, and the Tool-Changing/Photodetector Module. More detailed discussion of these items can be found in the respective Master's theses of two other MIT students.: Wen Kai Hsiao [Hsiao] and David Roberts [Roberts]. Of the remaining Toolbox Items, the sponsor company was to provide the Stripping Tool, the Cleaning Tools, and the Fusion Splicing Tool. This left the design of the two other toolbox items, the Cleaving tool and the Rejacketing tool, which were the author's primary design responsibilities.

2.2 Design of Tray Manipulation Module

2.2.1 Functional Requirements, Specifications and Constraints

The following are the functional requirements and specifications for the Tray Manipulation Module:

1. It must be able to accommodate rectangular component trays with maximum dimensions of 32 in x12 in.
2. It must be able to position tray holes with a repeatability of less than 0.010 in.
3. It must be able to operate at speeds grater than 2 in./sec.

The constraints on the Tray Manipulation Module are that the areas immediately above and below the tray surface must be open in order to not interfere with the movements of the Fiber Manipulation Module and the Photodetector Module.

2.2.2. Detailed Design Of the Tray Manipulation Module

The design chosen for the Tray Manipulation Module is illustrated in Figure 2.4. It is called the X-Z gantry concept for obvious reasons. It consists of two parallel belt driven linear stages (servo-driven and operating in a master-slave orientation) that carry a third linear stage in what will hence forth be referred to as the X direction. This linear stage in turn carries the actual tray. Together these stages can move the tray within a rectangular workspace measuring 30 in. by 70 in.

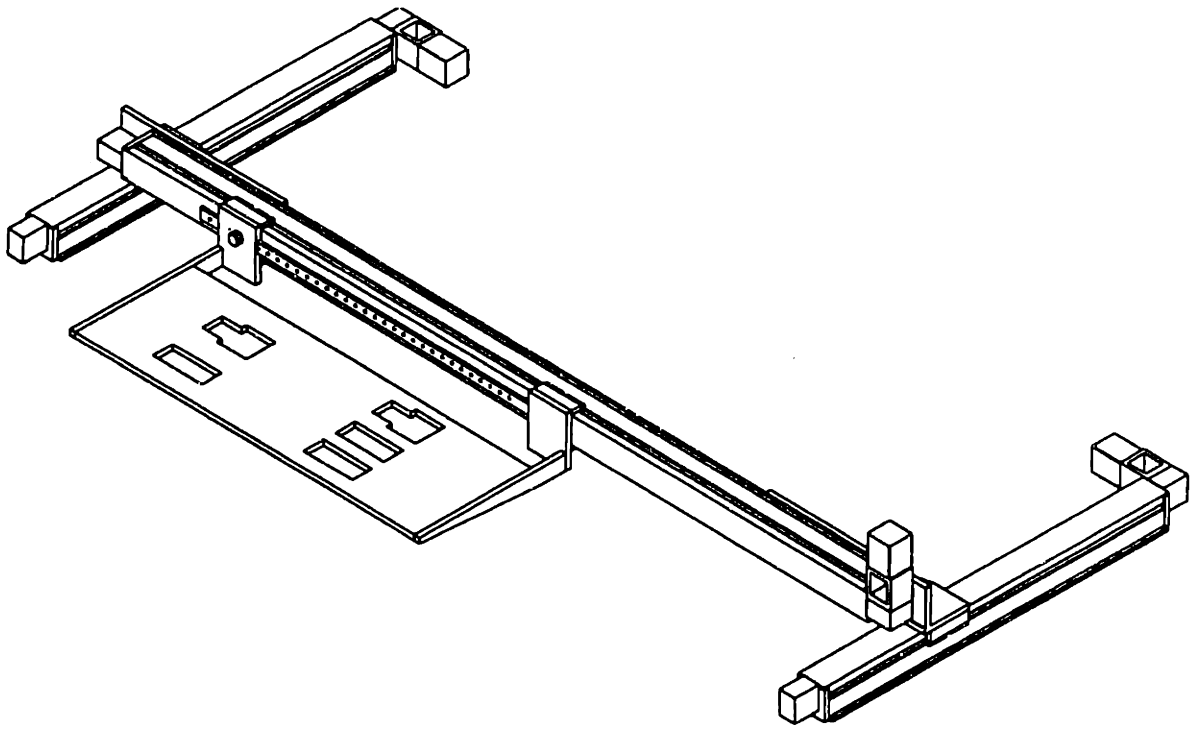

Figure 2.4: Detailed Design of the Tray Manipulation Module

2.3 Design of The Fiber Manipulation Module

2.3.1 Functional Requirements, Specifications and Constraints

The functional requirements, specifications, and constraints for the Fiber Manipulation Module are as follows:

1. It must be able to grasp fiber leads from the component tray and move them through a range of X = 1 in. (25.4 mm), Y = 1 in. (25.4 mm), and Z = 4 in. (101.6 mm), with corresponding resolutions X = 10 μm, Y = 10 μm, and Z = 0.2 μm.
2. It must be able to rotate fibers through +/- 190 degrees with 1.5 degree resolution.
3. It must be able to apply any specified tension to the fiber from 0 to 100 kpsi.

2.3.2 Detailed Design of the Fiber Manipulation Module

The final design for the Fiber Manipulation Module is shown in Figure 2.5. It consists of a five bar positioning mechanism that can position an object to the above X, Y, and Z specifications. Two servo motors operate in conjunction to move the five-bar in X, and Y, while the Z movements are controlled by a belt driven, servo-controlled linear slide. Affixed to this mechanism is a set of fiber grippers that open and close on a rack and pinion mechanism. A series of pneumatic actuators is mounted on the grippers to allow the opening and closing of them with varying force. The rack and servo-driven pinion also enable the two gripper pads to move parallel to one another while the pads are closed, resulting in the rotation of any fiber held in the pads. The Manipulators have locators that enable precise, repeatable placement of the fibers within the pads. Finally, the entire gripper mechanism is mounted to the five bar through a strain gauge flexure, so that any force on the pads can be measured.

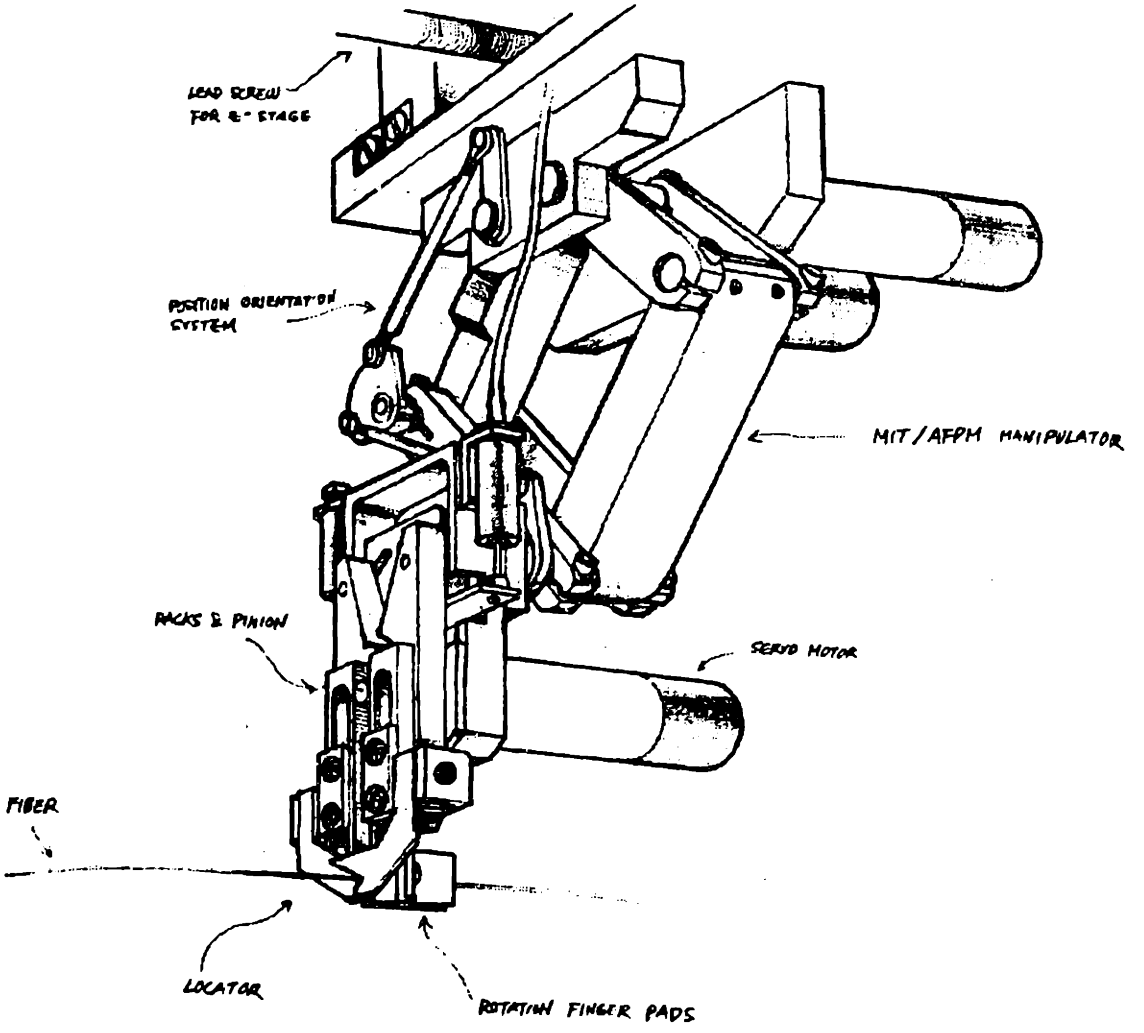

Figure 2.5: Detailed Design of Fiber Manipulation Module

2.4 Design of Tool Changing/ Photodetector Module

The designs of the Tool Changing Module and the Photodetector Module are presented together because, even though both originally were considered very different module, the final simplified OAS design makes one a part of the other.

2.4.1 Functional Requirements, Specifications and Constraints

The functional requirements of the Tool Changing Module are as follows:

1. It must position and raise each of the toolbox items into the work location so that they can work on fiber leads.
2. It must be able to raise the Photodetector and slide it into position over a fiber lead on a tray.
3. It must be able to position each tool with a repeatability of less than 0.005 in.(125 μm) in the X, Y, and Z directions.

2.4.2 Design of the Tool Changing Module

Figure 2.6 shows the detailed design of the Tool Changing Module. It consists of a number of Pneumatic band cylinders mounted on an aluminum carrier plate. This plate is in turn mounted to a servo-controlled linear stage. One of the band cylinders carries the Photodetector, and the others carry tool box items. The linear stage can maneuver each individual tool and the photodetector into a Z position underneath the fiber work location. After this, the band cylinders raise each tool in Y to the work location, where they perform their specific parts of the operation. The photodetector is actually an integrating optical sphere that when raised into a hole, can be further moved by the Tool Changing Module to dock and remain in its measuring position while its band cylinder returns to its down position, allowing for optical measurement while the Tool Changer is Maneuvering tool box items.

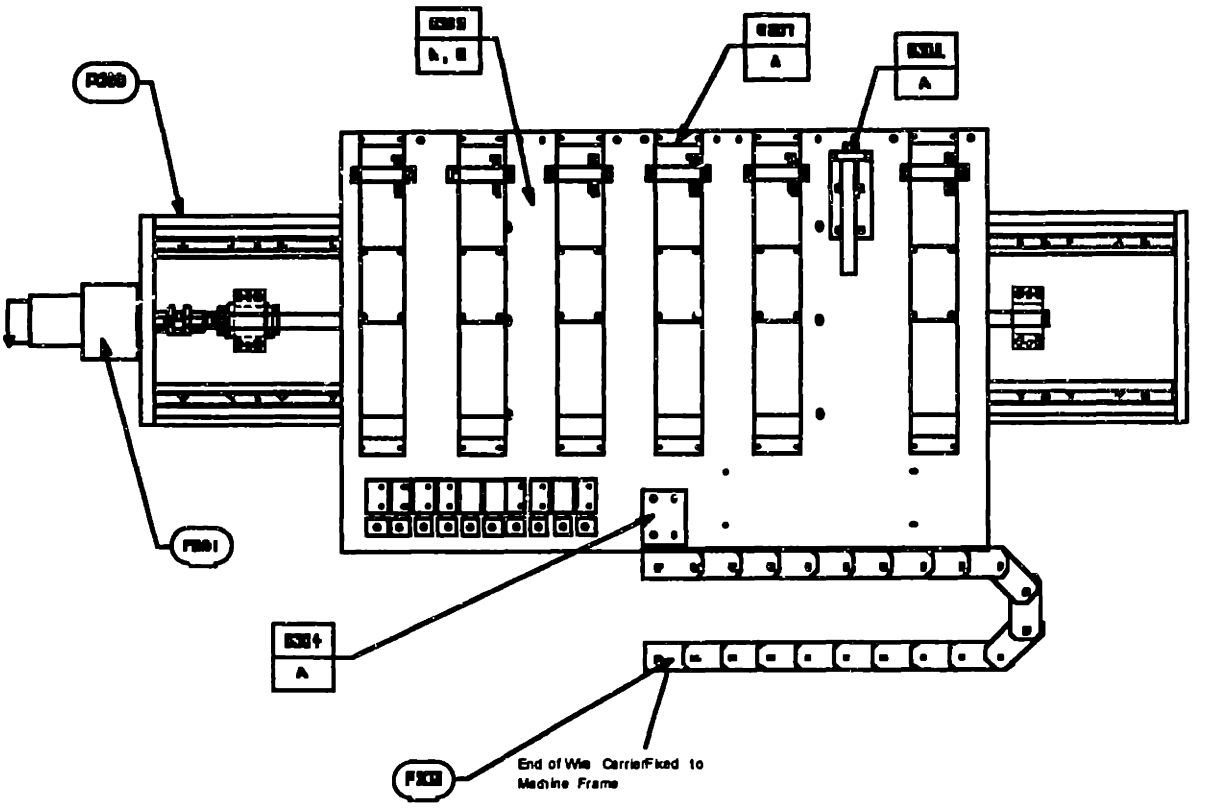

Figure 2.6 The Tool Changing Module

2.5 Overall OAS Design and Conceptual Process

Figure 2.7 shows the complete integration of the above components onto a machine frame.

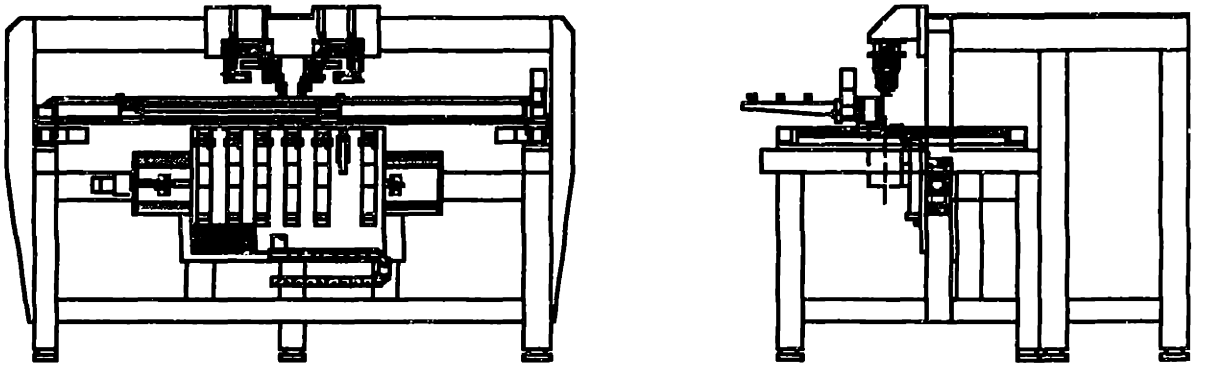

Figure 2.7: The Optical Assembly Station

In order to more easily understand the design choices primary to this research, the it is necessary to understand the OAS splicing process. Figure 2.8 shows a typical tray hole. Of note are the "Fiber Holders." These are essentially clamps that hold the fiber leads in place over the hole. They open and close to allow for fiber leads to be maneuvered to a splice. Also, note that the hole is asymmetric. This allows the photodetector to be raised through the hole and docked into position.

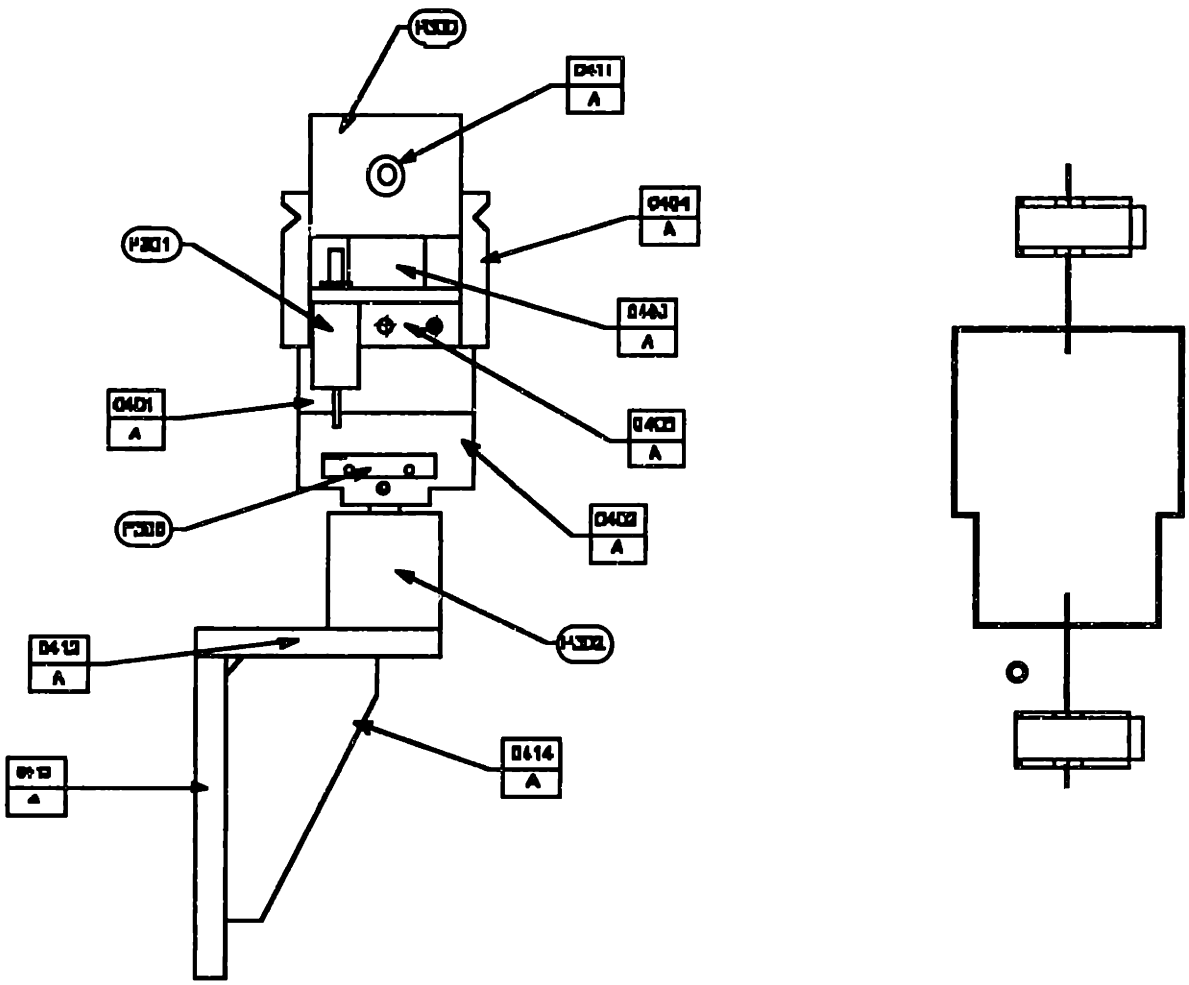

Figure 2.8: Photdetector and Typical Tray Hole

The following is the process conceived for a single hole on the OAS. Figure 2.9 follows to illustrate the steps. [Roberts, pp. 45-47]:

(a) The fiber leads are loaded onto the component tray and placed in the fiber holding blocks. The fiber holding blocks close tightly on the fiber so that the fiber does not move when the operator loads the tray onto the machine or when the OAS maneuvers it.

(b) Once the Tray Manipulation Module maneuvers the first tray hole to the work location, the Tool Changing Module positions the photodetector below the work location and raises it up through the tray hole. The fiber leads are separated enough so that the tool structure does not hit them.

(c) The Tool Changing Module linearly indexes the photodetector to the left to allow the fiber lead to slide inside the structure, and the detector takes a reading. The photodetector then docks to the tray, and the band cylinder carrying this tool is then recessed to its home position on the Tool Changing Module. In normal operation, this tray hole is then moved out of the fiber work location so that the tray hole where a splice is to be performed is moved into the fiber work location. Through all of the splicing operations at the up stream tray hole, the detector remains docked to the downstream hole, monitoring light intensity through the upstream splice. When all operations are complete at the upstream hole, the downstream tray hole is then brought back to the fiber work location. The band cylinder raises to contact the photodetector in the same position that it left it.

(d) The Tool Changing Module then linearly indexes the Photodetector tool back away from the fiber lead and pulls it down below the tray to its home position. The fiber leads at this hole are now ready to be prepared. The tray is maneuvered so that the new downstream hole is in the fiber work location and the photodetector is docked to this hole in the same manner as above. When it is docked, the tray is maneuvered so that the upstream hole is back in the fiber work location. The tray remains static until all fiber operations are performed at this location.

(e) Here the fiber leads are ready for fiber operations.

(f) The left fiber is the first to be prepared. Fiber Manipulator #1 (always responsible for the left fiber lead) descends from above the tray with the fingers and locator open. The locators close in order to accurately position the fiber, and then the fingers close to grasp the fiber. The box shown in the diagram includes both the locators and the fingers.

(g) The left fiber holding block opens to allow the manipulator to pull the fiber lead through the block, and over the tray hole.

(h) The fiber holding block closes and the manipulator fingers open. The fingers slide back to their original position, then close again on the fiber. The purpose of pulling the fiber out is to present enough lead for fiber operations to occur. The fiber holding block then opens.

(i) The Tool Changing Module Positions the Stripping Tool beneath the fiber work location under the left fiber lead and raises it to contact the fiber. The tool strips off a one inch long center portion of the fiber jacket. The Stripping tool is then recessed to its home position

(j) The Tool Changing Module Positions the Cleaning Tool beneath the fiber work location under the left fiber lead and raises it to contact the fiber. The one inch

long center stripped portion of cladding is then cleaned. When completed the tool is recessed to its home position.

(k) The Tool Changing Module Positions the Cleaving Tool beneath the fiber work location under the left fiber lead and raises it to contact the fiber. The cleaving tool cleaves the fiber, and recesses to its home position.

(l) Here all of the fiber preparation is complete for the left fiber lead.

(m-r) The process repeats for the right fiber lead. (Now the manipulator is #2)

(s) Here both fiber leads have been prepared and are ready for splicing.

(t) Both sets of manip[ulator fingers bring the fiber leads together until they are almost touching. The Tool Changing Module positions the Splicing Tool beneath the center of the fiber work location and raises it to the fibers. The Splicing tool then performs the fine alignment of the fibers (communicating with the manipulator fingers to perform the rotation and long axis movements) and fuses the fibers together). The tool then recesses to its home position.

(u) The Manipulators apply tension to the fibers for prooftesting.

(v) The Tool Changing Module positions the Rejacketing Tool beneath the center of the fiber work location and then raises it to contact the splice. The tool rejackets the fiber, and then recesses to its home position.

(w) The Fiber Procedure at this hole location is complete, and the power loss is measured.

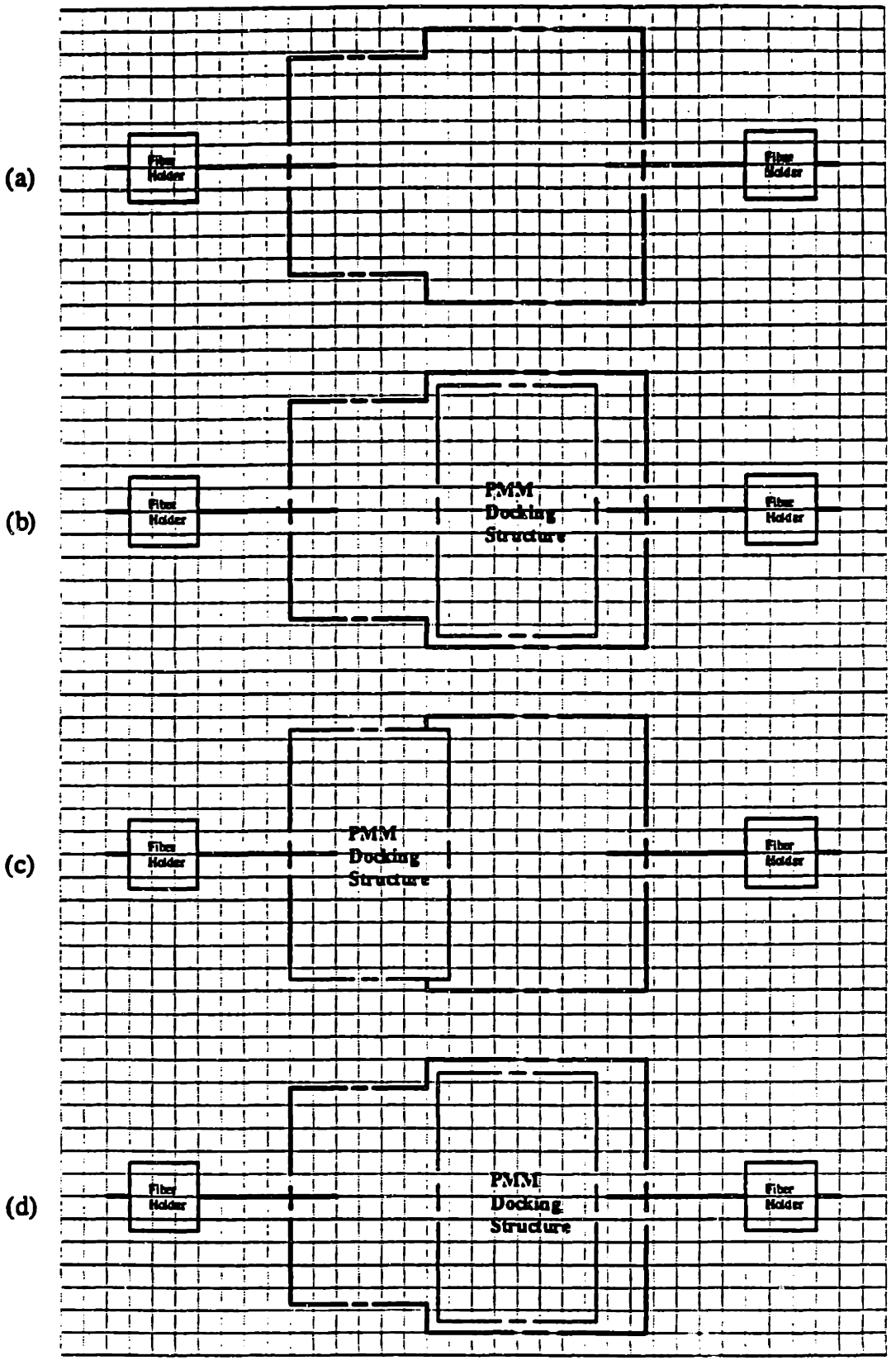

Figure 2.9: Conceptual OAS Process

(e)

(f)

(g)

(h)

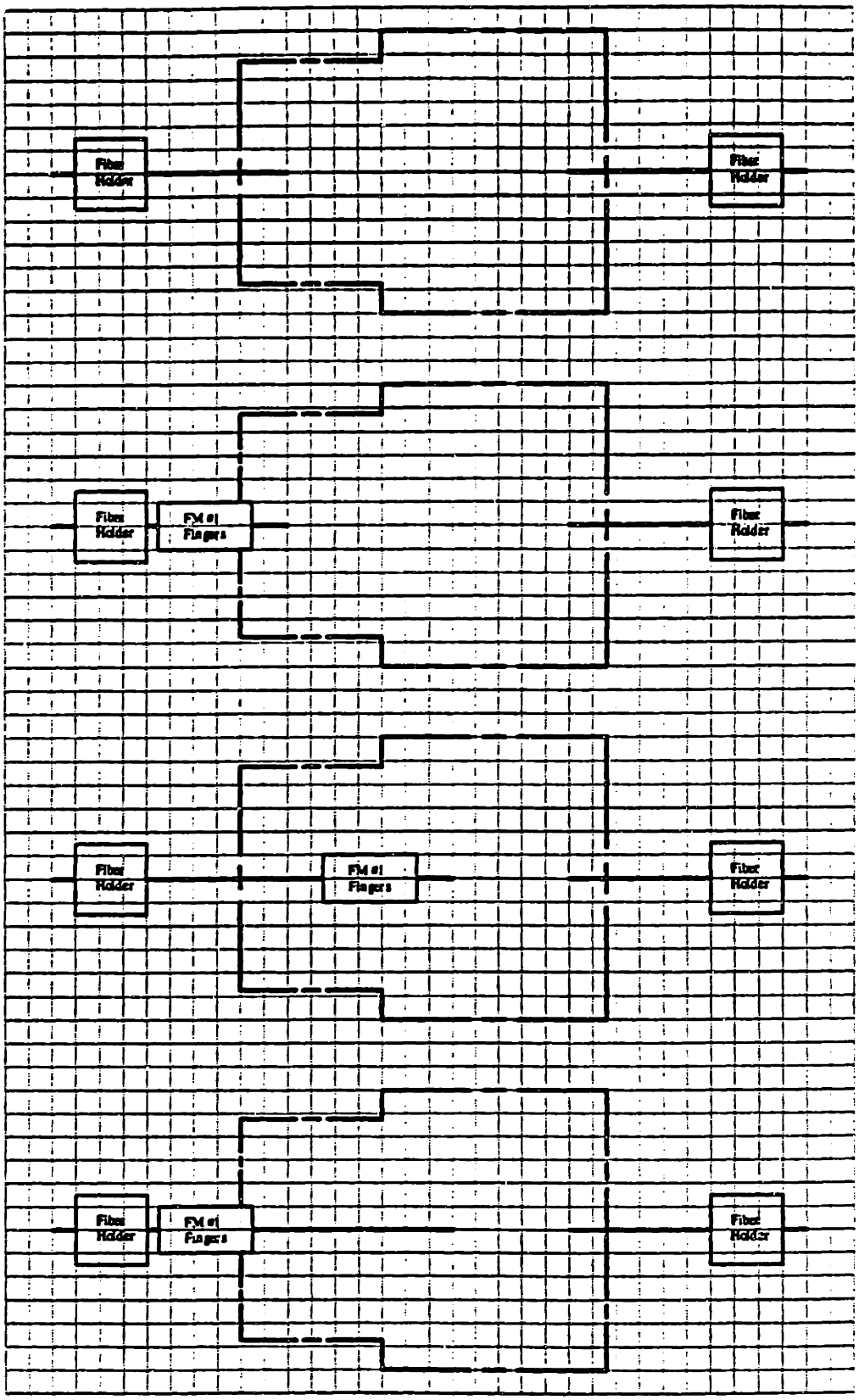
Fiber Holder
Fiber Holder
Fiber Holder
FM of Fingers
Fiber Holder
Fiber Holder
FM of Fingers
Fiber Holder
Fiber Holder
FM of Fingers
Fiber Holder

(i)

(j)

(k)

(l)

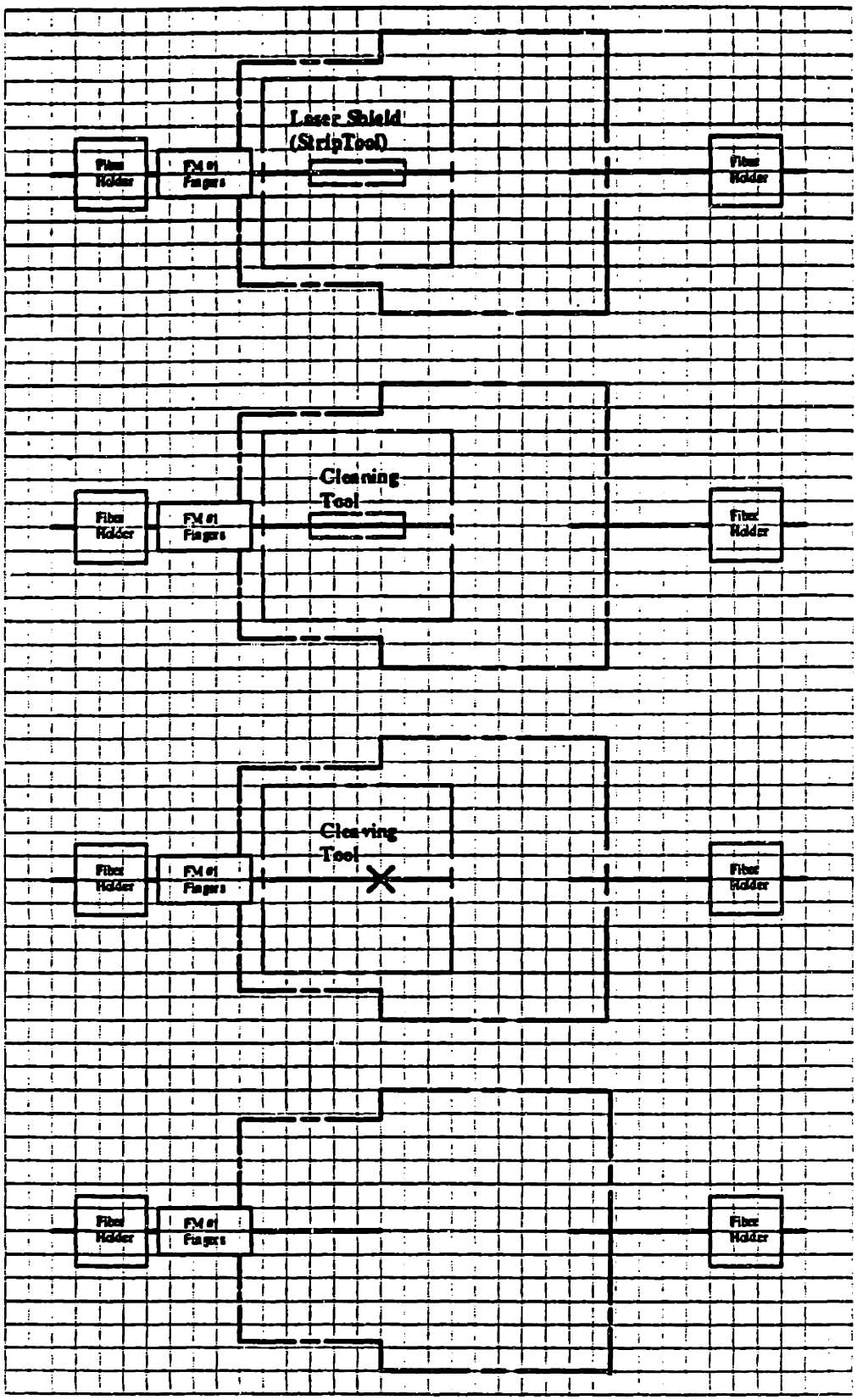
Laser Shield
(StripTool)
Fiber Holder
FM of Fingers
Fiber Holder
Cleaving Tool
Fiber Holder
FM of Fingers
Fiber Holder
Cleaving Tool
Fiber Holder
FM of Fingers
Fiber Holder
Fiber Holder
FM of Fingers
Fiber Holder

(m)

(n)

(o)

(p)

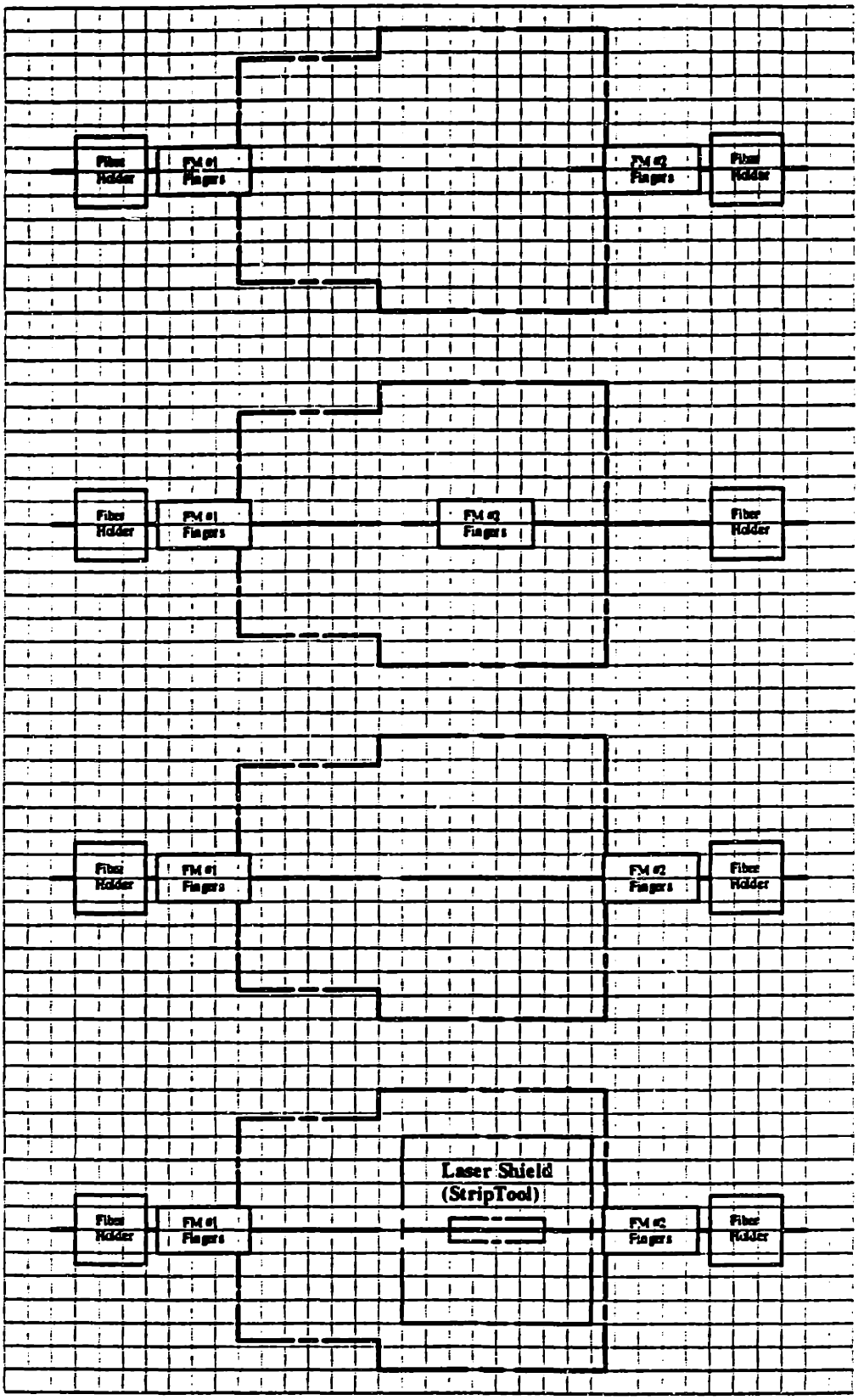

(q)

(r)

(s)

(t)

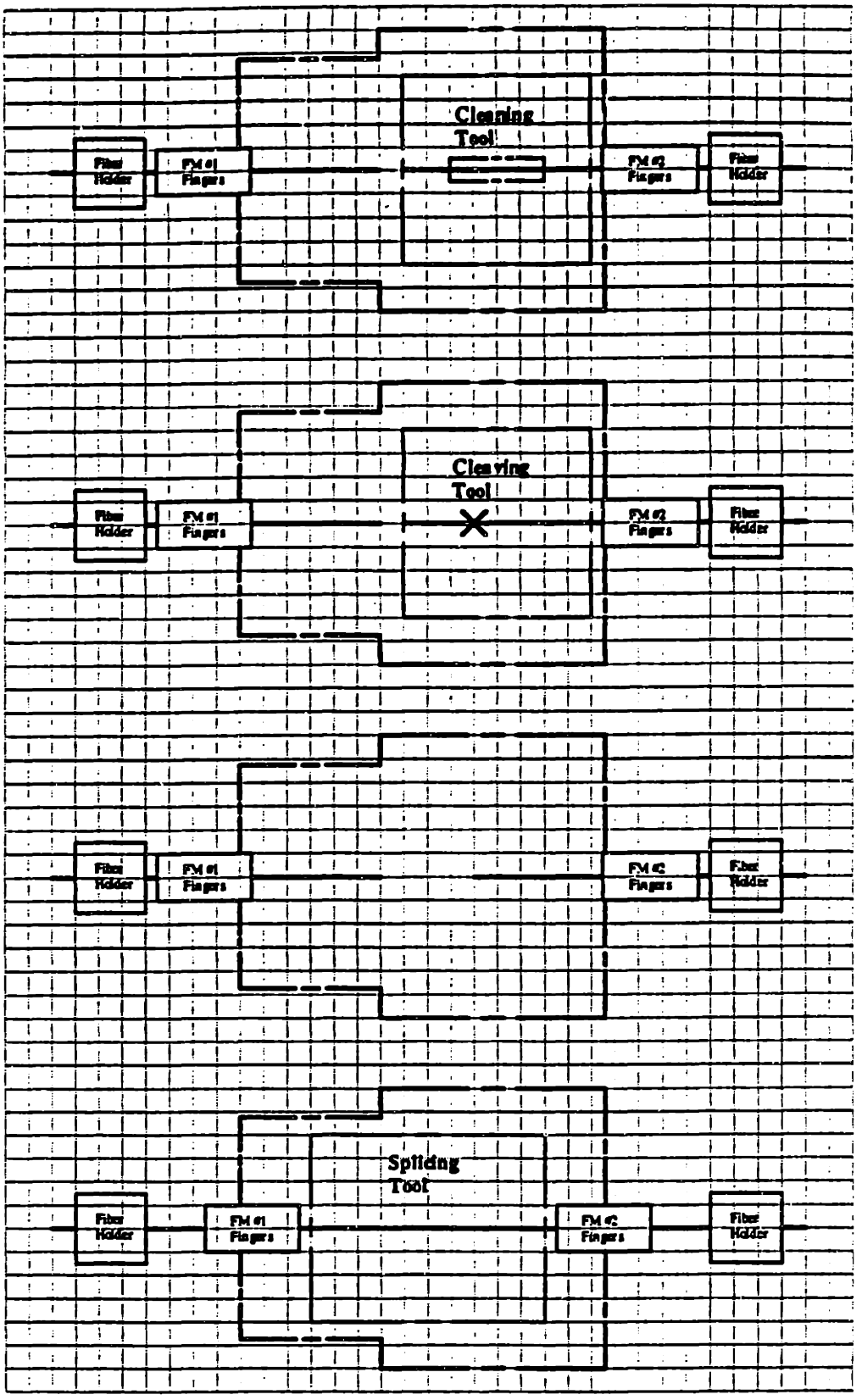
Cleaning Tool
Fiber Holder
FM #1 Fingers
FM #2 Fingers
Fiber Holder
Cleaving Tool
Fiber Holder
FM #1 Fingers
FM #2 Fingers
Fiber Holder
Fiber Holder
FM #1 Fingers
FM #2 Fingers
Fiber Holder
Splicing Tool
Fiber Holder
FM #1 Fingers
FM #2 Fingers
Fiber Holder

(u)

(v)

(w)

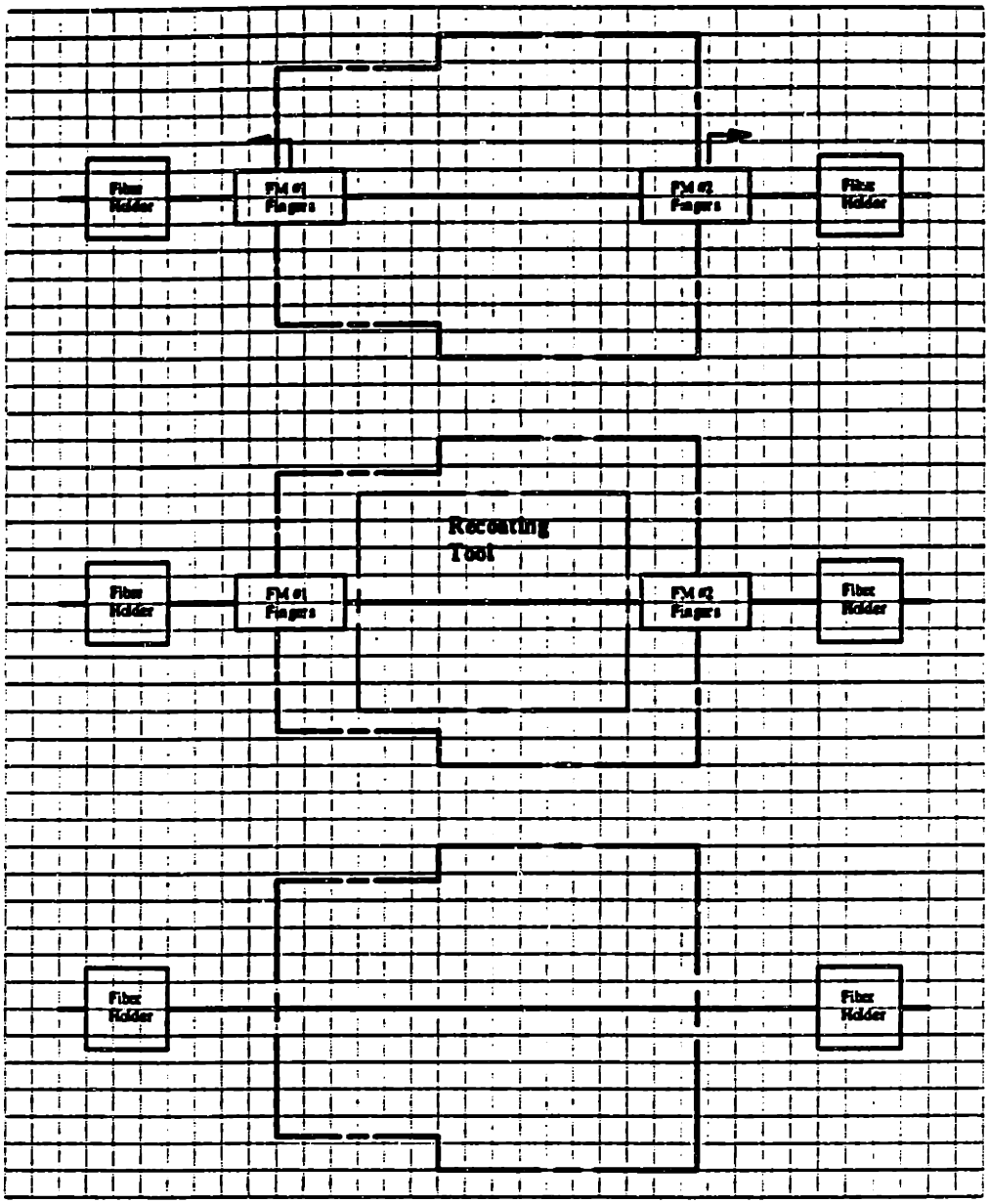
Fiber Holder
FM of1 Fingers
FM of2 Fingers
Fiber Holder
Recoating Tool
Fiber Holder
FM of1 Fingers
FM of2 Fingers
Fiber Holder
Fiber Holder
Fiber Holder

2.6 Conceptual Design of Cleaving Tool

2.6.1 Functional Requirements, Specifications and Constraints

The functional requirements, specifications, and constraints for the Cleaving Tool are as follows:

1. It must be able to produce consistent smooth fiber end faces with less than 2 degrees of end angle.
2. It must be able to accommodate fiber jacket diameters of 135 μm, 165 μm, and 225μm, as well as cladding diameters of 80 μm, and 125 μm.
3. It must have a variance in length of its cleaved fibers of no more than 400 μm.
4. It must be able to cleave both the right and left fibers at a given hole.

Functional requirement number one mandates that the Cleaver must be able to propagate a crack perpendicular to the fiber that results in cleaved surfaces that have no cracks or irregularities. Most manual cleaving tools in existence do this by applying tension along the long axis of the fiber and nicking the cladding surface with an extremely sharp object. This results in a surface crack that, if the tension is uniaxial and of the right magnitude, quickly propagates perpendicularly through the cladding and leaves a smooth endface. It was decided that the Cleaving tool would employ such a technique.

The second functional requirement, that the Cleaver handle a variety of fibers, greatly influences its design. In order to attain a good cleave with the tension and nick technique, the sharp object should graze the fiber from the side and the surface crack must be on the order of a few microns (see Figure 2.10) . Having different fiber sizes means that the point of contact between the sharp object and the fiber cladding would vary from fiber to fiber. This means that position of the blade would have to change for each fiber type.

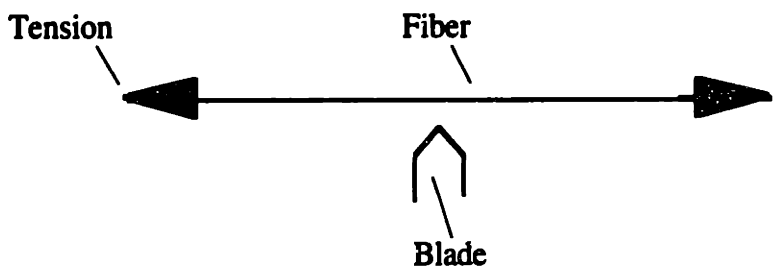

Figure 2.10: Cleaving

The third functional requirement is process related. The alignment for the fusion splicing is done with CCD camera vision feedback. In order for its software to recognize fibers, they must have their cleaved endfaces facing each other in a window of 800 μm. If the length of any cleaved fiber varies from its nominal length by more than 400 μm, it may be out of the range of the Splicing Tool's CCD. This means that the tensioning mechanism for the Cleaver cannot let the fiber slip more than 400μm during the cleaving procedure.

The final functional requirement involves the geometry of the tool. Because each tray hole has a fiber lead on both sides, the cleaving tool (and, indeed, all of the toolbox items) has to be symmetric with respect to the tray hole.

2.6.2 Design Selection

At the point just prior to cleaving in the OAS process, the manipulator has a center-stripped fiber in its grippers. Because the cleaving process requires tensioning, it was desired to have the Cleaving Tool work in Conjunction with the Manipulators. For this reason, it was decided that the Cleaving Tool would consist of two grippers with a blade centered between them. Depending on which fiber (left or right) is being cleaved one gripper would close on the jacketed end of the fiber lead, and the manipulator would tension from the other end,

leaving the stripped and cleaned cladding exposed above the blade. The only remaining hurdle was how the blade was actually going to make contact with the fiber.

The most readily available blade was a circular diamond-tipped cutting wheel used in many existing fiber optic cleaving tools. If the cleaver was to use the same grippers for all fiber diameters, then the physical place where the blade needs to strike changes by .002." An outside company working closely with MIT on the project had developed a technique that would solve the blade interface problem. Their idea was to mount the diamond wheel .005" off an actuated axis of rotation. Figure 2.11 shows this eccentric cleaving wheel concept. During one full rotation of the wheel, its top edge translates a full .01" in the vertical. If a tensioned fiber is aligned properly above the wheel, and the wheel is made to ratchet back and forth through a rotation (moving, say, 5 degrees clockwise, and then 4 degrees counterclockwise 360 times), then the diamond edge will graze any fiber .010" or less from it in the desired manner.

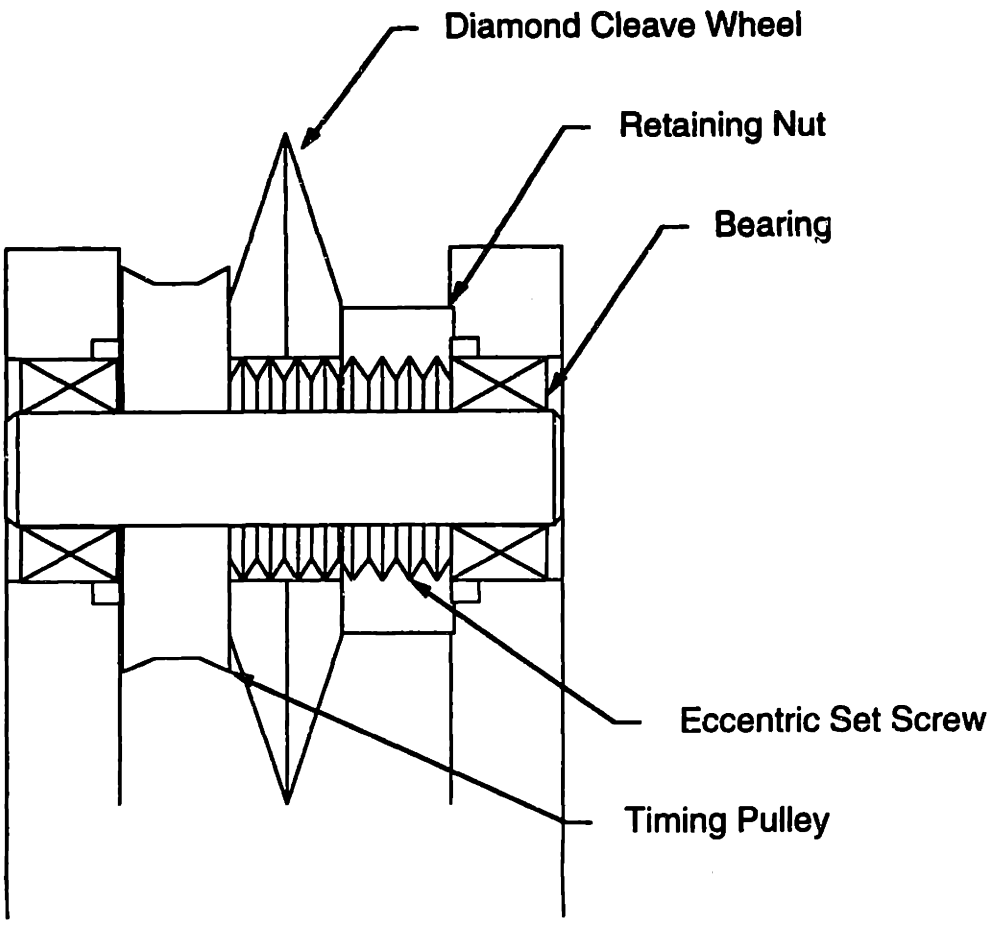

Figure 2.11: Eccentric Cleaving Wheel Concept

2.7 Conceptual Design of Rejacketing Tool

2.7.1 Functional Requirements, Specifications and Constraints

The functional requirements, specifications, and constraints of the Rejacketing Tool are as follows:

1. The Tool must apply and cure a uniform coating of acrylate to a 1.5" section of bare cladding.
2. The Tool must accommodate jacket diameters of 135 μm, 165 μm, and 225μm.
3. The tool must be able to rejacket an entire tray's worth of fiber with no human intervention (i.e. cleaning).

Functional requirement number one mandates that the Tool cover the entire surface of the cladding with UV curing epoxy, and then have some mechanism for curing the area with UV light. The coating is desired to be as much like the original jacket as possible, with no air bubbles or voids of any kind. A perfectly round rejacket is preferable, but some minimal irregularity or flash is acceptable.

The second Functional requirement is quite a stumbling block. Most existing Manual rejacketers are essentially molds that close over a given fiber size. fill with epoxy, and cure. For different sized fibers, different sized molds are employed. It adds a level of complexity to whatever tool is to be designed.

The final functional requirement concerns automation. The epoxy used to rejacket fiber is extremely sticky and viscous. All current manual rejacketers require extensive manual cleaning after *each* application. For MIT's rejacketing tool to conform with the time constraints imposed by the Sponsor Company, the tool would have to at least perform seven rejackets in a row (the most possible number of tray holes for a given tray) with no human maintenance.

2.7.2 Design Alternatives

The first concept explored is known as the "Open Mold" concept. The idea, illustrated inFigure: 2.12, is to fill a linear groove of some geometry and a depth on the order of a fiber diameter with epoxy, and then lower the fiber into it and apply UV light to cure it. The hope was that the fiber could be placed into the groove in such a way as to uniformly coat it, and that the process of curing would force all of the epoxy to leave the mold with the rejacketed splice. Also, in order to recoat fibers of varying diameter, one would need

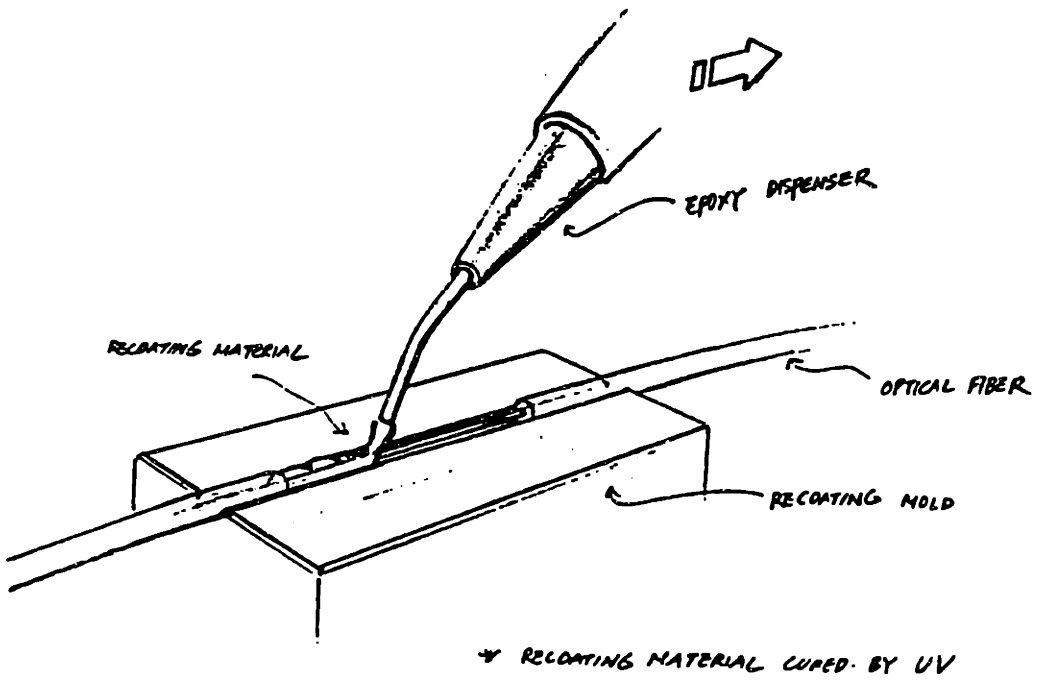

Figure 2.11: Open Mold Rejacketing Concept

only to fill the groove with varying amounts of epoxy. A series of tests were performed in order to attempt to prove the "Open Mold" concept. Three different geometry's of groove (rectangular, v-shaped, and circular) were machined into a number of different materials (including quartz, rubber, Teflon, aluminum, plastic, and steel). Also both a volumetric and pressure dispenser were used to fill these grooves. Although there was some success with a circular groove in quartz filled with a volumetric pump, no scenario yielded consistent results. The most common problems occur when attempting to remove the rejacket from the mold. Often the fiber tends to stick in the mold, due to the epoxy bonding with surface imperfections and the corners of the groove. Also, neither dispenser consistently delivers a bubble free dispense, causing the rejacket to simply break near the void area upon retrieval.

A second concept is a rejacketer with two halve circle grooves that close and seal around the spliced area. This concept would closely resemble current manual ricottas, where epoxy is injected into the cavity once the molds are closed, only it would have to seal much more effectively. Figure 2.12 illustrates the closed mold rejacketer concept. The concept is to have two half molds, one made of aluminum and the other of quartz, mate with each other over a fiber. In order to seal, rubber is placed along the aluminum end as close to the actual groove as possible. Once closed, an injection channel in the aluminum side is used to fill the mold. A UV source is located behind the quartz plates. The idea is that, since both ends of the mold are open, that it is possible to push enough epoxy through the mold to force out any air bubbles. Further, because the UV light only cures the area immediately around the groove, and not the ends, the result would be a uniform recoat with a small amount of flash. The design would allow for epoxy to leak out of the sides. The justification for this is that this epoxy would not cure, and therefor remain in liquid form throughout several splices, and be easily cleaned after an entire tray. A prototype closed mold rejacketer was built to show proof of concept, and yielded promising results. For these reasons the "closed mold" concept was selected.

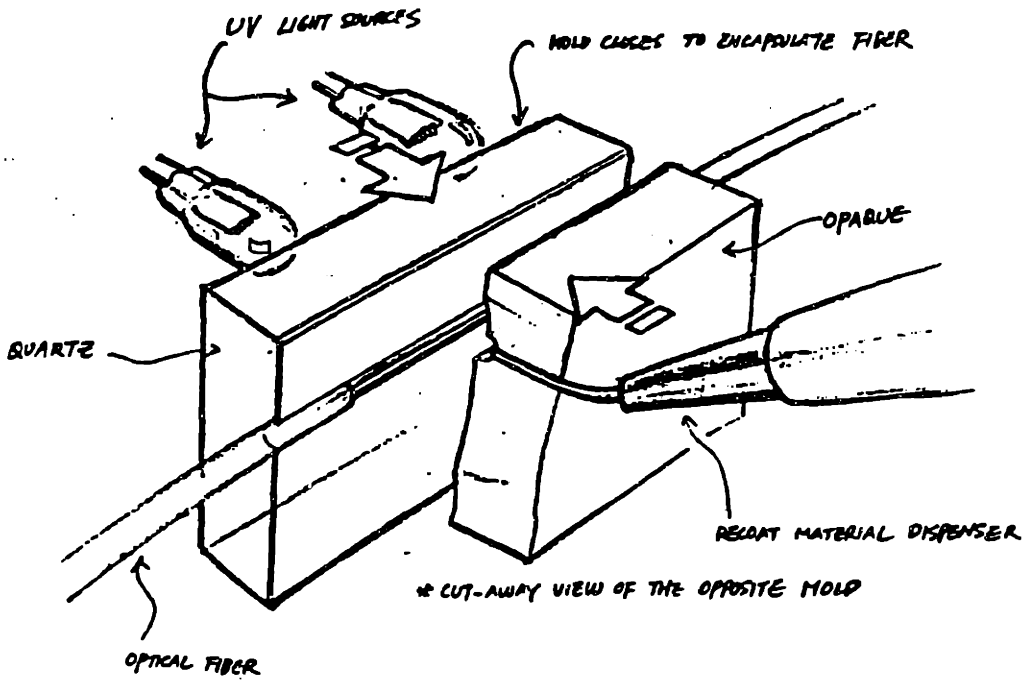

Figure 2.12: Closed Mold Rejacketing Concept

Chapter 3

3. Detailed Design of Cleaving Tool

This chapter begins with a more in depth overview of the cleaving technique and the requirements for a good fiber optic cleave. A brief review of the "eccentric cleave wheel" concept chosen for further development follows. The primary issues for completing the detailed design are then discussed in detail. The chapter concludes with a summary of the detailed design of the Cleaving Tool.

3.1 Overview of Cleaving Technique

3.3.1 Fiber Alignment

The first requirement for a good fiber optic cleave is fiber alignment. Ideally, the fiber to be cleaved should be exactly perpendicular to the plane of the cleave wheel. Any angle that the cleave wheel's scribe makes with the plane perpendicular to the long (Z) axis of the fiber is going to be the angle of the crack that propagates through the cladding and the resulting end angle of the cleaved fiber. Figure 3.1 demonstrates this phenomenon, showing both misalignment in X-Z and Y-Z planes. This means that over a nominal 2 in. of fiber length, the point to point placement of the

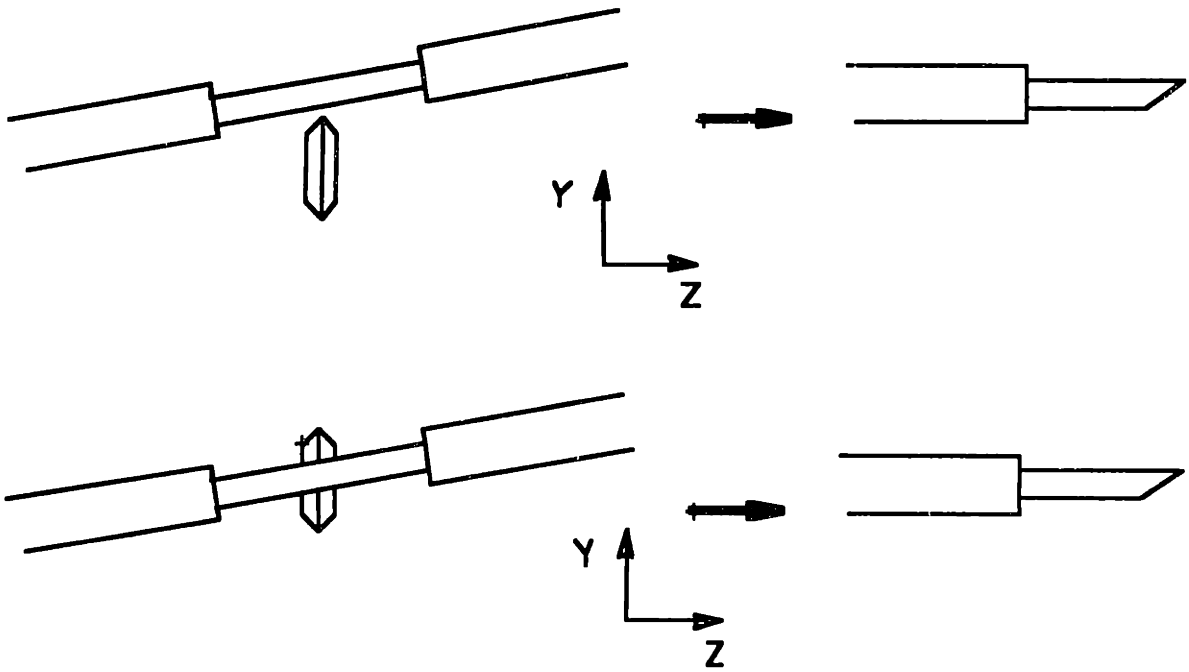

Figure 3.1: Effect of Fiber Alignment on Cleave Angle

fiber ends cannot be off more than .07 in. in either the X or Y directions in order to have a cleave angle of less than 2 degrees. Assuming that the Cleaving Tool gripper always holds the fiber in a fixed location, it is clear that the fiber Manipulators (with an X resolution of 10 μm, and a Y resolution of 10 μm) should be able to position the fiber repeatably for cleaving.

3.3.2 Tensioning

The second requirement for a good cleave is the type and amount of tension applied to the fiber. As discussed in Chapter 2, it is vital that the tension is applied on the long axis of the fiber only. Any bending moment or torsion applied to the fiber will affect the cleave angle and endface topography. Figure 3.2 demonstrates this. If any bending moment or torsion is applied , then

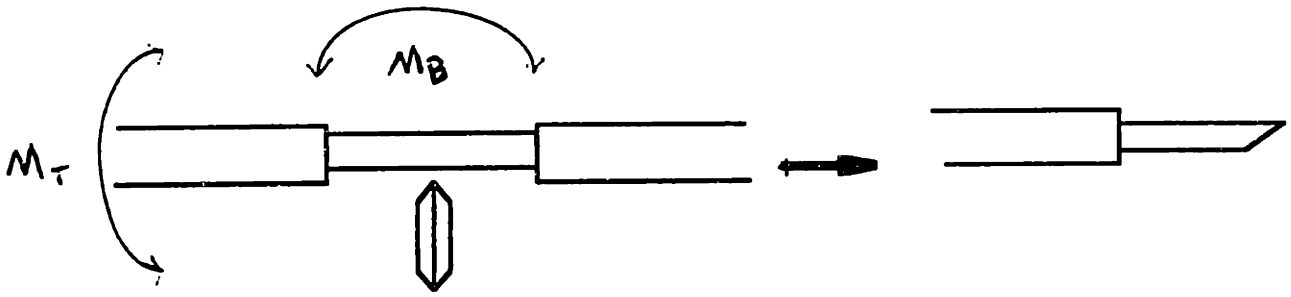

Figure 3.2: Effect of Moments on Fiber Cleaving

the result is a high cleave angle. This is because the local stress distribution at the scribe plane (assuming proper alignment) becomes uneven. This effects the path that the propagating crack follows through the fiber. Instead of moving directly up through the fiber, the crack spreads faster through the regions with higher stress. This can also result in uneven surface topography of the cleaved ends. This means that the pads holding the fiber must be parallel to it, and apply no twist.

The amount of tension applied to the fiber also greatly influences the cleave quality. Because the fiber must be held from the outside, it is virtually impossible to eliminate all moments on it, and there is a threshold value of nominal stress that must be achieved in order to overcome these moments. In general , a nominal stress of 18 MPa is needed for a good fiber optic cleave. This obviously suggests that a larger diameter fiber will need higher tension. Any stress lower than this will yield cleaves with the characteristic discussed above. If the tension becomes higher than the nominal value, the end angle becomes better, but the topography of the endface begins to change. When the stresses are to high, the cleave occurs due to a number of localized failures, intstead of one continuous crack.

3.2 Review of Conceptual Design

As discussed in Chapter 2, the "eccentric cleave wheel" concept was the one chosen for further development. This concept incorporates a set of grippers that work in conjunction with the fiber manipulators to align and tension the fiber over a cleave wheel. This cleave

wheel is mounted with its center a small distance off the axis of its rotation. The wheel is then turned through a rotation in successive forward and backward jumps (more degrees in the forward jumps), eventually just grazing the fiber during one of these jumps. The following is a list of issues that require further investigation in order to develop the concept into a detailed design:

1. volume constraints imposed by the Tool Changing Module and The Tray Manipulation Module
2. gripper pad geometry and placement
3. gripper actuation
4. cleave wheel actuation

These issues are discussed in detail in the following section.

3.3 Detailed Design Issues

3.3.1 TMM/TCM Volume Constraints

The existing OAS design played a fundamental role in deciding the geometric configuration of the Cleaving Tool. As is evidenced in the process outline in Chapter 2. each of the Toolbox Items either works to prepare both the left and the right fiber leads for splicing, or works with both leads at the same time. The preparation tools must operate on both the left and right sides of the fiber work location, while the splicing, and rejacketing tools are raised to the center of the location. As the tray remains stationary throughout the process at a single hole, size of the tray hole obviously has a major impact on the parts of the tools that must be raised through the tray. Also, the width of the carrier plate on the Tool Changing Module determines the maximum allowable widths of the Tools on it. Finally, the depth below the tray of the docked Photodetector, as well as the length and stroke of the

band cylinders on the Tool Changing Module determine the maximum overall height of any tool. Figure 3.3 shows the volume constraints that

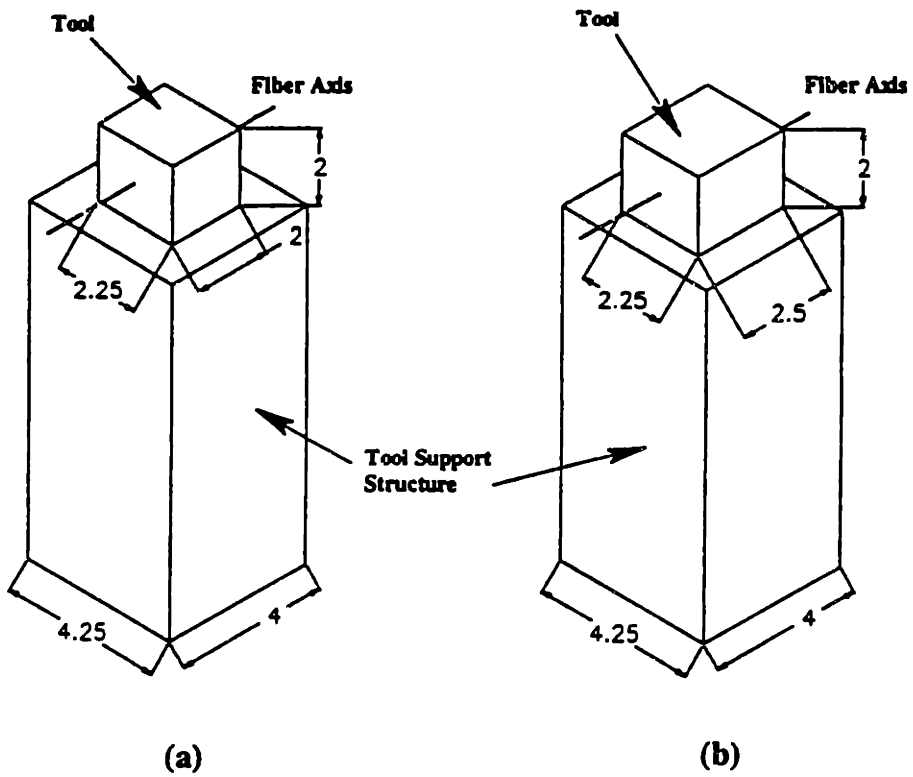

Figure 3.3: TMM/TCM Volume Constraints
(a) Dual Position Tool (b) Center Position Tool

result from the above considerations. Being a dual position tool, the Cleaving Tool has to limit its above tray geometry to a box with base dimensions of 2 in. x 2.25 in. and a height of 2 in. This means that the housing of the cleave wheel eccentric, and the grippers on either side have to be less than 2 in. wide and 2.25 in. long. Also, its below tray X-Z dimensions must fit with thin a rectangle 4 in. wide by 4.25 in. thick. This means that the motor that turns the Cleave wheel, as well as the mechanism that opens and closes the grippers, have to be restricted to this space. The reader will notice that Figure 3.3 gives no overall height dimension, as this was not known precisely at the onset of the Cleaving Tool's Design. Although the length and stroke of the band cylinders were known, the tools could be mounted on the band cylinders in a variety of ways, and up to six inches

below the band cylinders could be utilized as needed. As an outside company was currently beginning work on the splicing tool, the overall height constraint was still being negotiated. Considering this, as well as the remaining detail design issues, it was decided to limit the overall height of the Cleaving Tool to 8 in.

3.3.2 Gripper Pad Geometry and Placement

The OAS process mandates that the grippers on the cleaver be able to align and hold a fiber lead that has .5 in. of jacket, followed by a 1 in. section of stripped, cleaned cladding, and cleave off .25 in. of this cladding to leave a prepared fiber lead with .75 in. of cleaved cladding. As the pre-designed housing for the eccentric has an overall width of .75 in., and it is desired that the grippers have at least .0625 in. of clearance from the side of the housing. This leaves a total of 1 in. to accommodate the width of both grippers, or .5 in. for each. Within this space there needs to be some mechanism to precisely align the fiber, as well as some area where the fiber lead can be held tightly for tensioning. Figure 3.4 shows the selected gripper design. Each gripper set has two

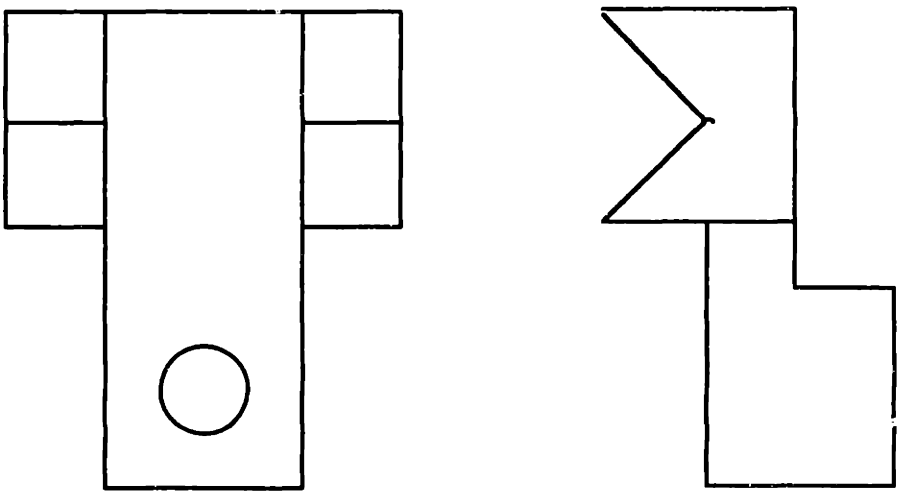

Figure 3.4: Gripper Design

mating pieces. The first being a flat with v-grooves on either side. The depth of the V-grooves extends slightly below the flat. When the second piece, which is simply a flat, closes over a fiber against the first, the v-grooves serve to align the fiber precisely in the gripper, until it is gripped, when they no longer touch or torque the fiber in any way. Both flats are micro-sand blasted to ensure a strong frictional hold on the fiber.

3.3.3 Gripper Actuation

The grippers should open wide enough to accept the fiber leads, and close with enough force to hold them. The first part of the above statement may seem trivial, as the largest fiber diameter is only 225 μm. It should be noted, however, that there often exists in fiber leads a phenomenon known as curl. This occurs when the fiber has been wound into some radius, (such as that of the spools that fiber is sold on) and the jacket has retained some memory of this radius. The result is a slight bend in the fiber leads, varying with the history of each lead, that makes their exact position above any of the preparation toolbox items unknown. For this reason, the fiber grippers should open to the fullest extent with respect to the above tray volume constraints. The detailed design for the gripper actuation shown in Figure 3.5 meets this requirement as well as the closing force requirement, by pivoting two arms that hold the grippers, and actuating

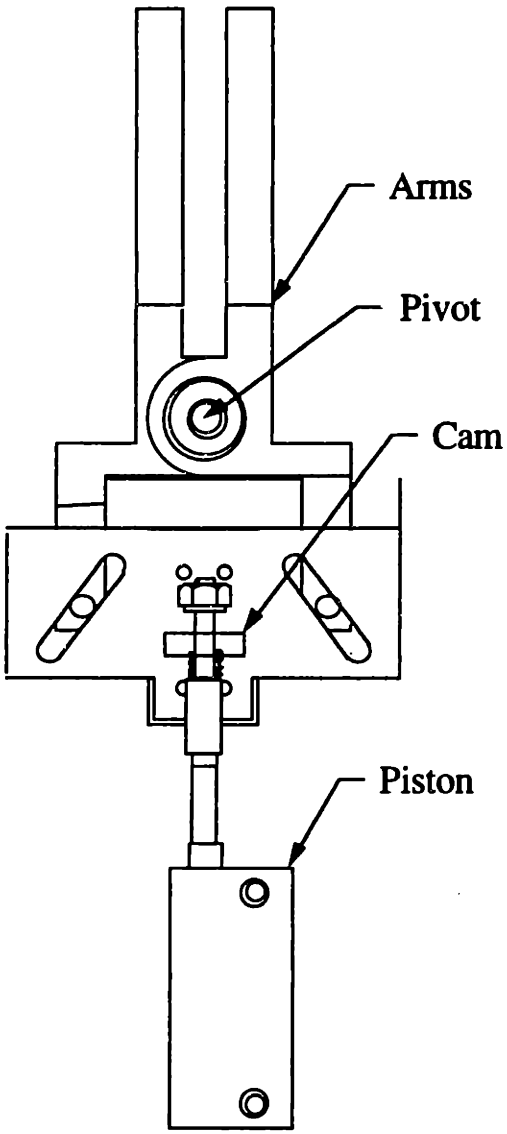

Figure 3.5: Gripper Actuation

these arms pneumatically through a cam. The length of the arms above the pivot (2.5 in.)was chosen to open the grippers as wide as possible, while the bore of the pneumatic cylinder driving the cam was chosen to deliver enough force to hold the fiber under tension (at 70 psi., about 3.5 lbs.). The piston is also flow controlled, to ensure a smooth opening and closing of the grippers. Because of the desired aspect ratio for the arm, they were made of stainless steel to minimize deflection. The cam is made of bronze, and the sliding pins are hardened steel, to eliminate stiction, and the need for applied lubricant.

3.3.4 Motor Selection

The final detail design issue is the choice of actuation for the cleave wheel. A more in depth look at the cleaving algorithm is needed to motivate motor selection. As stated in Chapter 2, the eccentric mechanism should be able to ratchet back and forth through a rotation as quickly as possible. The actual cleaving algorithm only moves the wheel through a half of a rotation. The wheel begins in its lowest vertical position. It is then moved 5 degrees clockwise and 4 degrees counterclockwise 180 times. At this point, the wheel is in its highest position, and should have come into contact with the fiber, thus cleaving it. It then recesses to its home position. The control package for the OAS, can accommodate both servo and stepper motors. Of these choices, a stepper motor was chosen because it has enough torque to handle the constant direction changes quickly, and one could be found small enough to fit within the below tray volume constraints.

3.4 Summary of Detailed Design

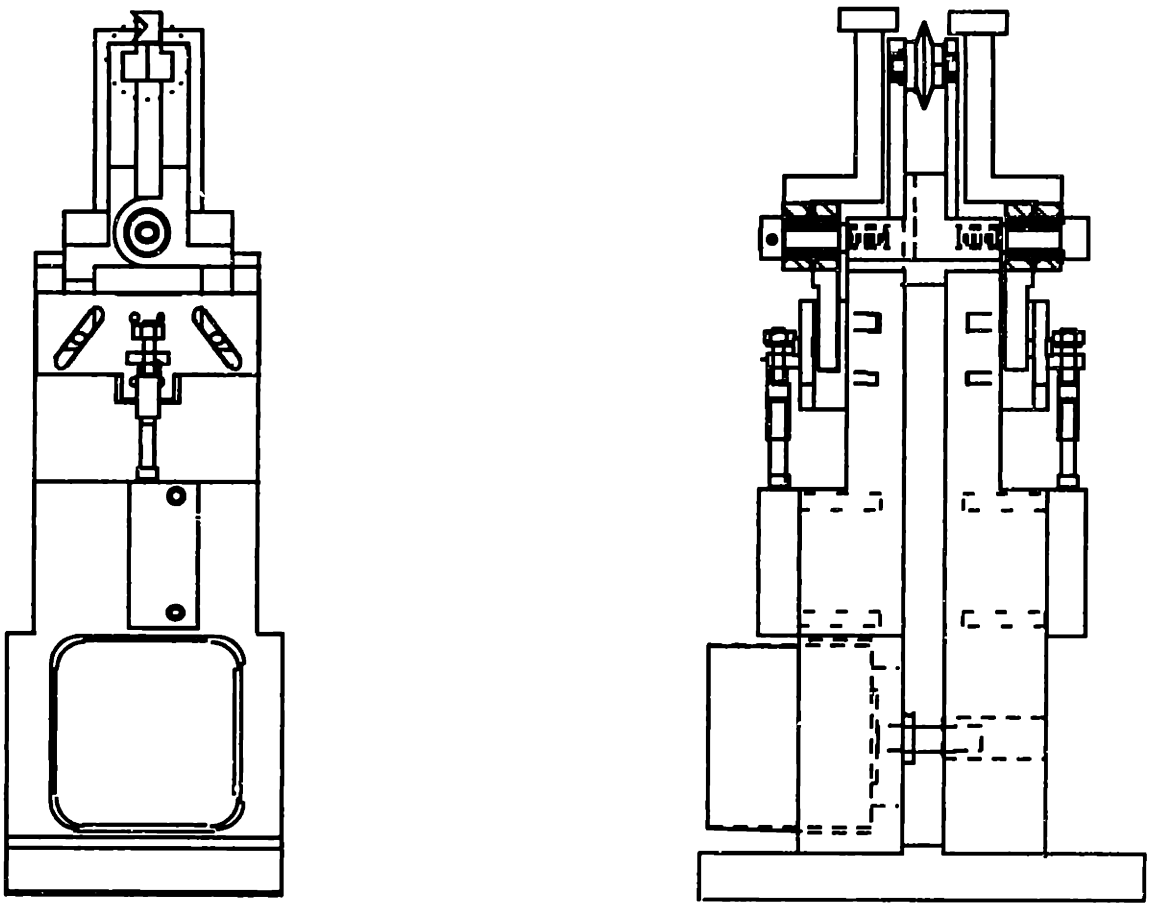

Figure 3.6: Detailed Design of the Cleaving Tool

Figure 3.6 shows the final Detailed Design of the Cleaving Tool. The tool is completely symmetric with the exception of the stepper motor mounted on one side. Note that the motor is at the bottom and actuates the cleaving wheel through a timing belt that runs through the center of the frame. The side mounted pistons actuate the grippers as discussed above.

Chapter 4

4. Detailed Design of a Rejacketing Tool

4.1 Review of Conceptual Design

As discussed in Chapter 2, the "closed mold" concept was the one chosen for further development of the Rejacketing Tool. The concept incorporates two half-circle molds that seal around the unjacketed fiber, are filled with UV curing epoxy, subjected to UV light to form a permanent rejacket, and opened to allow for the removal of the fiber. One of the molds is machined into an opaque material and has a channel leading from it to allow for epoxy insertion. The other is machined into quartz glass to allow for light to pass into the curing area. The molds are held in actuated housings that allow for their functions. The housing for the opaque mold allows for the epoxy to enter, and the housing for the quartz mold allows for placement of a source of UV light. In addition to similar volume constraints as those discussed for the Cleaving Tool in Chapter 3, (refer to Figure 3.3(b), as the Rejacketing tool is a Center Position Tool), there are a number of issues that require further investigation for this conceptual idea to be developed into a detailed design. They are as follows:

1. opaque mold specifications
2. quartz mold specifications
3. fiber location
4. housing design and actuation

These issues are discussed in detail in the following section.

4.2 Detailed Design Issues

4.2.1 Opaque Mold Specifications

The functional requirements for the Rejacketing Tool stated in Chapter 2 that the tool had to accept spliced fibers with a 1.5 in. stripped section and jacket diameters up to 225 μm. For this reason, both mold halves are 1.625 in. long, and greater than 125μm deep. The first specification concerning only the opaque mold is its material. Because the mold has a filling channel machined directly into the side of the very small half circular groove, the material needs to be strong enough to have very thin walls in places, and must be easily machined. Since aluminum posses these characteristics, and is also a good reflector of UV light, it is the material of choice for the opaque half of the mold. If this half is to seal with the quartz half, it must have a ledge on either side of its groove to allow for the placement of a condensable rubber seal. Finally, the half mold needs clearance holes to allow for fastening into the housing. Figure 4.1 shows the design of the Aluminum Half Mold.

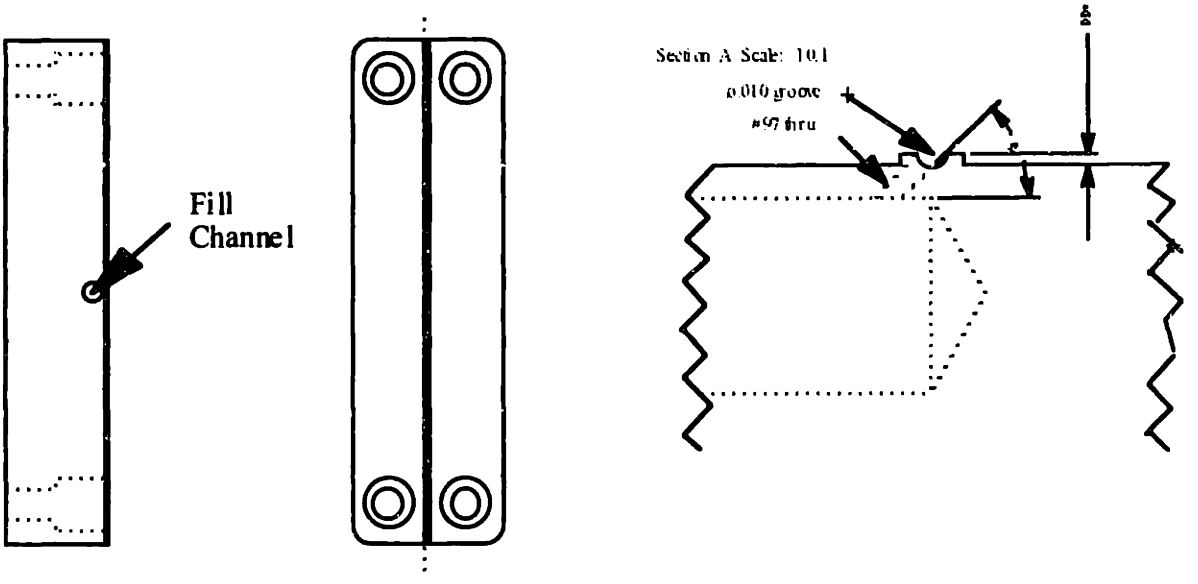

Figure 4.1: Aluminum Half Mold With Blowup Of Fiber Groove and Shelf

4.2.2 Quartz Mold Specifications

There are two important characteristics for the quartz mold half. The first is the surface roughness of the half circular groove. It is important for the groove to be as smooth as possible so that when the epoxy cures, it will not tend to bond with the groove. The smoother that the groove is, the easier it is to remove the fiber. The second important characteristic is that the area on either side of the groove be as flat as possible. This is because this area must form a seal with the rubber on the aluminum half. For these reasons, the groove surface is polished, and the face of the mold is ground optically flat. Also, to ensure that the brittle quartz does not break and that both molds seat flat against each other when closed, a layer of rubber is placed between each and its respective housing. Figure 4.3 shows the design of the quartz half mold.

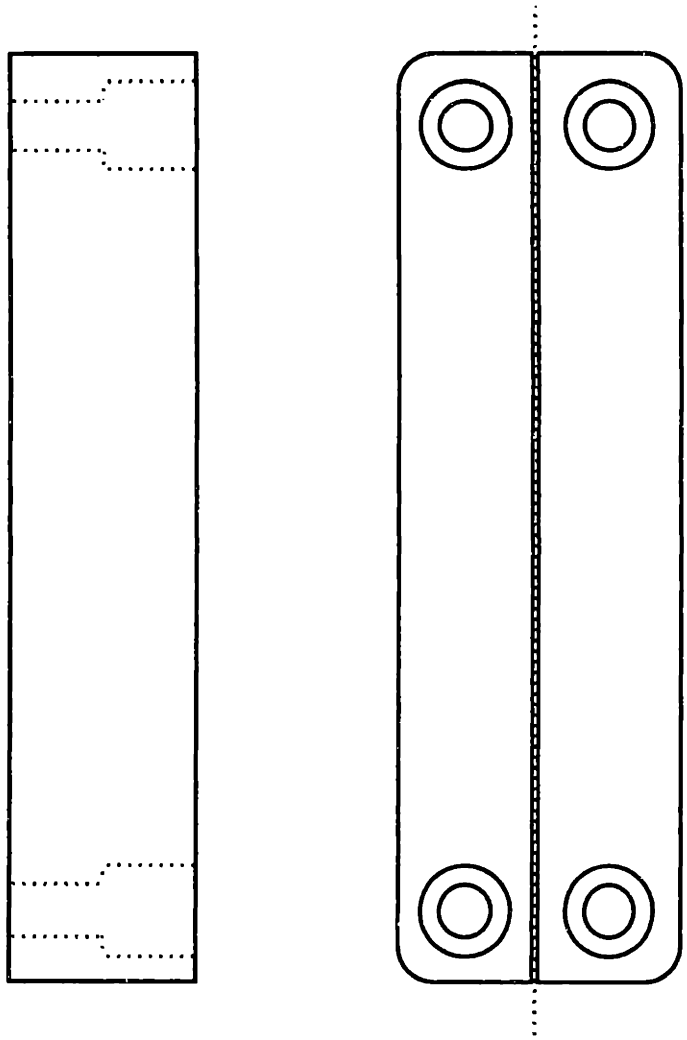

Figure 4.3: Detailed Design of Quartz Half Mold

4.2.3 Fiber Location

In order to accurately guide the unjacketed fiber into the molds, it is necessary for these molds to have locators that allow for any slight fiber misalignment. Figure 4.4 shows a set of these locators. They employ a similar v-groove design to that of the Cleaving Tool grippers, where the bottom of the alignment groove is just below the bottom of the fiber groove. The difference here is that each half mold has two locators that mate with the other's when the mold is closed Because there is compression involved in the closing of the mold, the locators must be fixed on each mold half. For this reason, each mold half has mounting slots on either side.

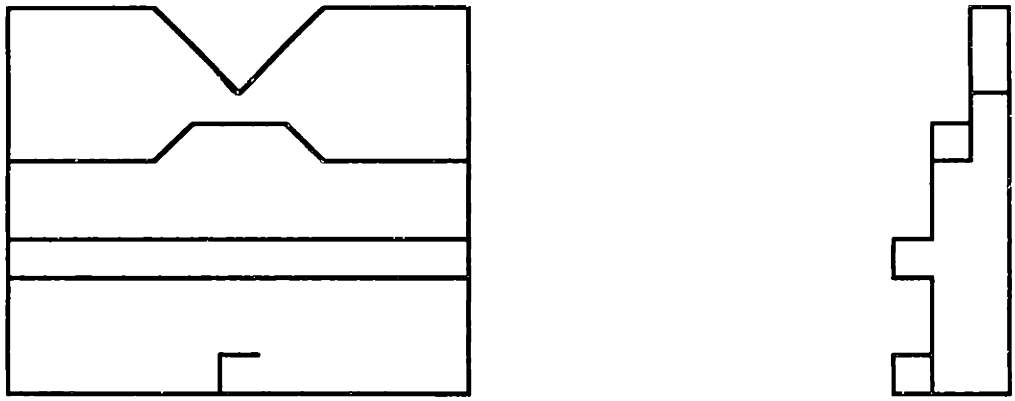

Figure 4.4: Fiber Locators

4.2.4 Housing Design and Actuation

The detailed designs of the housings for the quartz and aluminum mold halves are shown in Figures 4.5 and 4.6, respectively. The quartz housing has a pocket to allow for the placement of the mold, and three sockets to accommodate halogen lamps. Although these lamps emit about 98% white light, they exhibit enough UV to cure the small amount (about 900 μl) of epoxy needed for a rejacket. There is also a slot to allow the light to pass into the quartz mold. The aluminum mold housing also has a pocket to allow for the placement of the mold. Instead of light sockets, it has a clearance hole to enable the epoxy dispenser tip to be pressed into the fill channel of the aluminum mold.

In order for the locators of the mold to mate properly, the two housings must remain parallel as they open and close. For this reason, they are actuated via a four bar linkage. Figure 4.7, which shows the overall design of the Rejacketing Tool, illustrates this linkage. Each Housing is pivoted on the four bar, with stops to ensure that the molds do not open farther than the Volume constraints allow. In addition, tapered dowels emanating from the Quartz Mold housing mate with alignment holes on the Aluminum Mold Housing to ensure that they properly align during closing. The entire four bar linkage is actuated via a cam mounted on a guided pneumatic cylinder. The outer linkages are connected via an

extension spring such that the molds are normally open, and can be closed with the force of the piston.

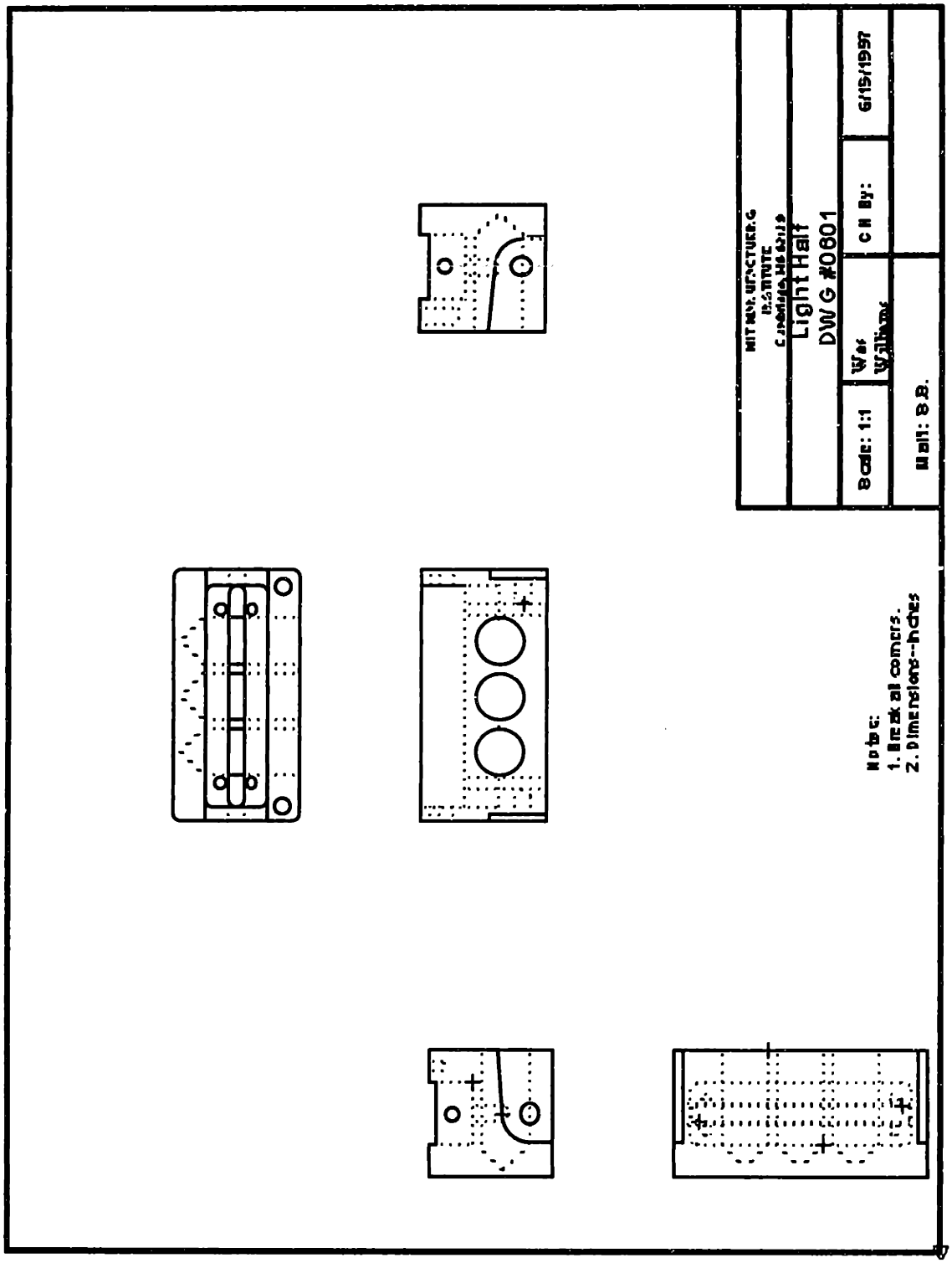

Figure 4.5: Quartz Housing

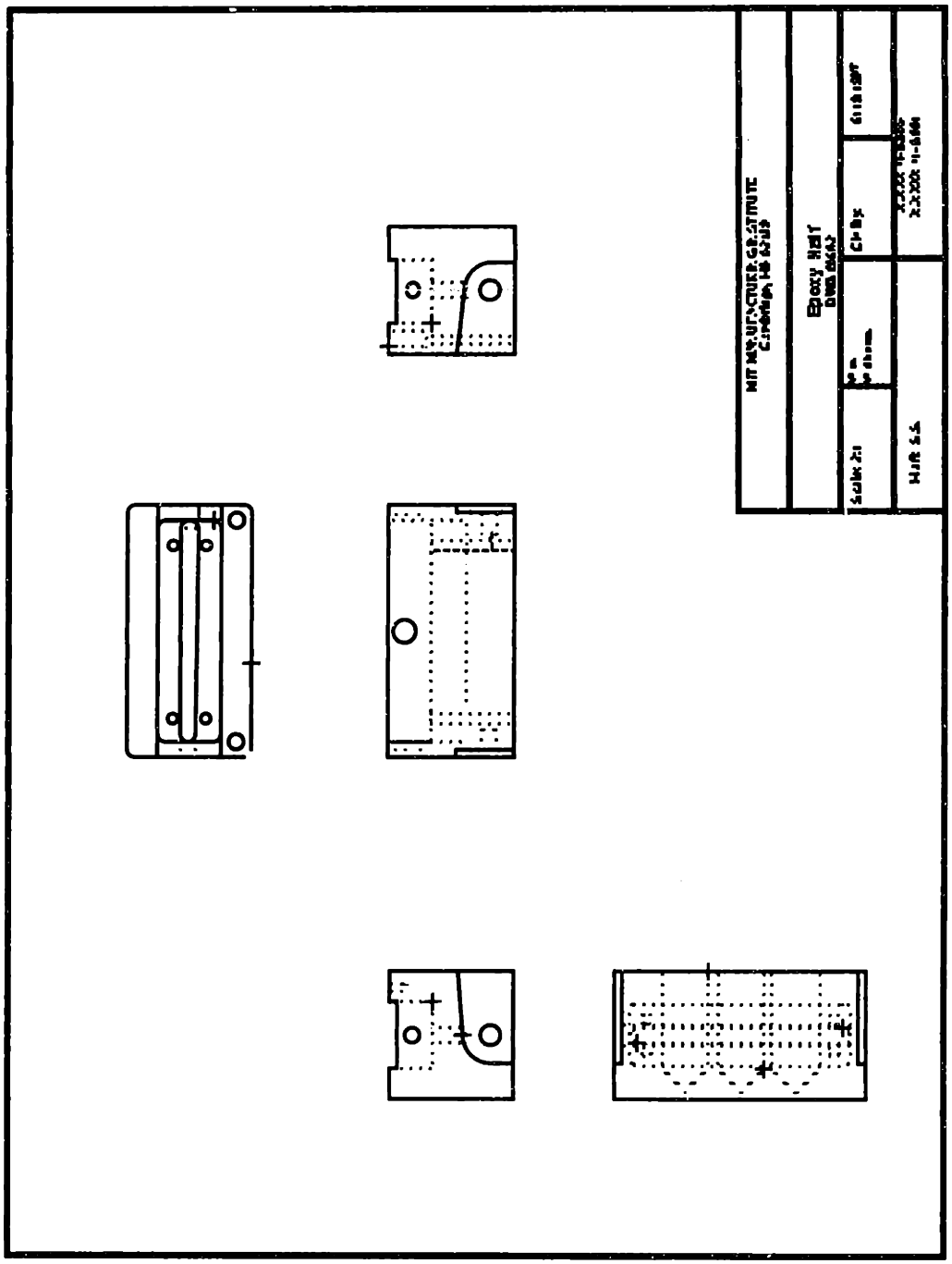

Figure 4.6: Aluminum Housing

4.3 Summary of Detailed Design

Figure 4.7 shows the overall design of the Rejacketing tool. Mounted as a center position tool on the Tool Changing Module, the Rejacketing Tool is normally open in its recessed position on the Tool Changing Module. After the spliced fiber is positioned by the Fiber Manipulation Module, the Rejacketing Tool raises. Its Piston actuates to close the molds. As it does, the fiber locators guide the fiber into the half circle grooves. Once the Mold is sealed the epoxy dispenser fills the channel with UV curing epoxy. The halogen lamps then light for a approximately 20 sec. Next, the piston releases, and the molds are opened by the force of their spring. A rejacketed fiber emerges from the mold.

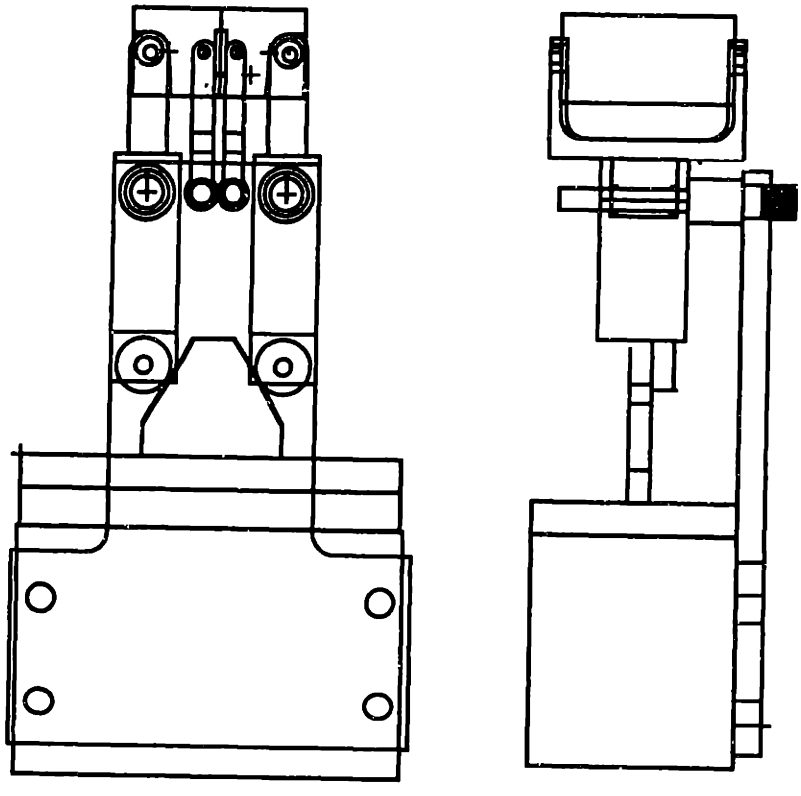

Figure 4.7: Detailed Design of Rejacketing Tool

Chapter 5

5. Toolbox Item Testing

This Chapter discusses the testing done in order to ensure the compatibility of three of the Toolbox Items with the other OAS modules and the OAS process. Two of these tools are the Cleaving Tool and the Rejacketing Tool, which were discussed in previous chapters. The third is the fusion splicing tool that has been provided by an outside vendor.

5.1 Cleaving Experiments

In order to prove the functionality and repeatability of the Cleaving Tool, the sponsor company mandated that the tool produce 30 continuous small core single mode cleaves and 30 continuous PM cleaves, with less than 5% of these having poor surface topography or a cleave angle of greater than 2 degrees. In these tests, it was desired to mimic the actual OAS conditions as closely as possible. At the time of their execution, however, it was impossible to align and tension the fibers with the Fiber Manipulation Module (as none existed), so an experimental setup was created.

5.1.1 Experimental Setup

The experimental setup for the cleaving tests is shown in Figure 5.1. It consists of the Cleaving Tool, a pulley of adjustable height, a set of gram weights, and several center-stripped sections of optical fiber. The Cleaving Tool was fastened to ground with the clamp, and the pulley was aligned with it such that a gripped fiber could lay over it and be aligned in X, Y, and Z, perpendicular to the cleave wheel. A number of the gram weights (90 g for SM and 80 g for PM) were then attached to the free end of the fiber,

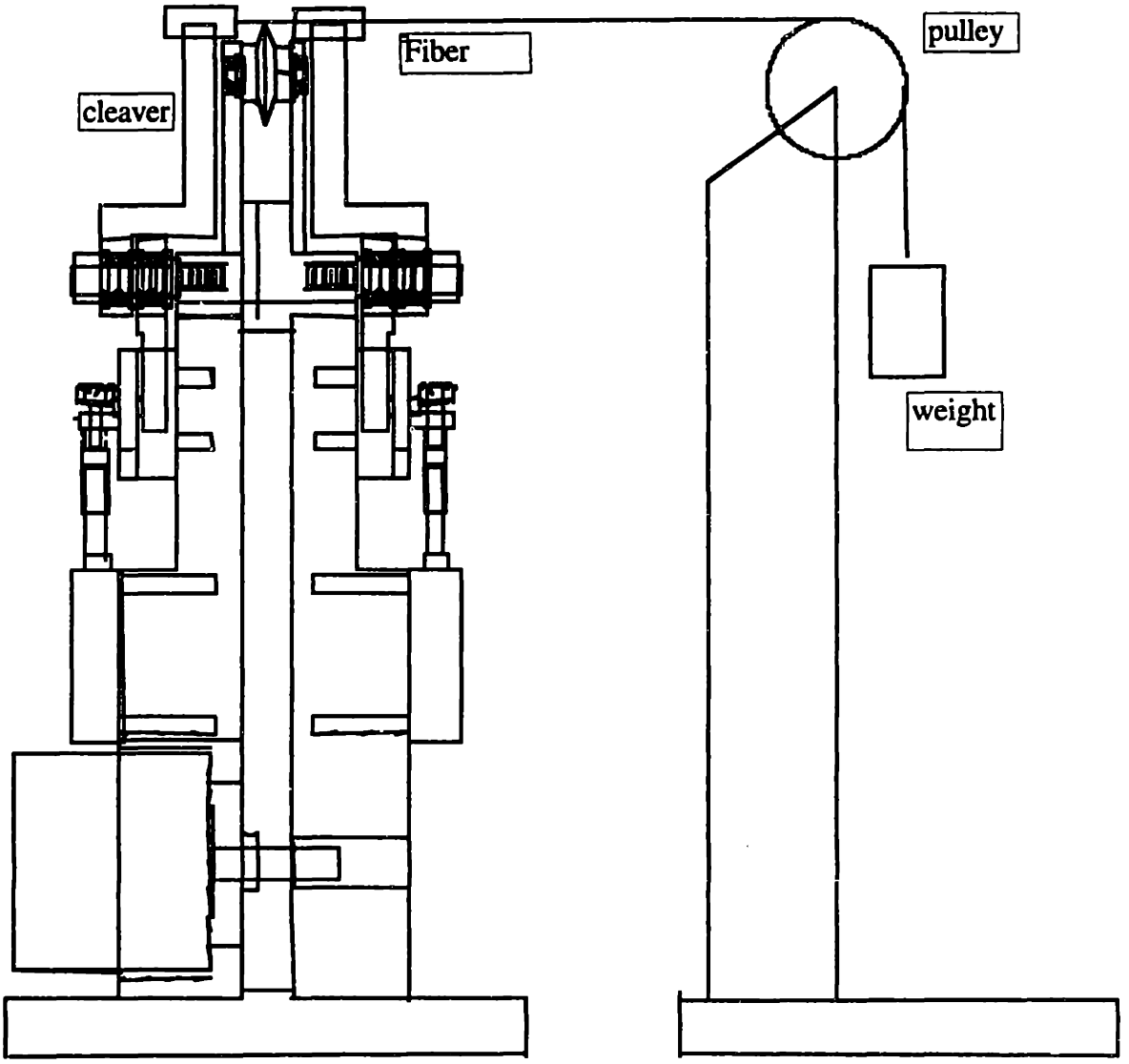

Figure 5.1: Experimental Cleaving Setup

and allowed to hang over the pulley. When the fibers were both aligned and tensioned, the Cleaving Stepper routine was initiated, and the fibers were cleaved. During these experiments, care was taken to ensure that the hanging weights remained as still as possible, so that the amount of torsion on the fiber was minimal (recall Chapter 3).

5.1.2 Cleaving Results

After the 90 cleaves were generated, they were collected and inspected with a cleave check interferometer. This devise uses the end face of a cleaved fiber as a mirror in a laser interferometer. The angle of this mirror with the horizontal determines the amount of interference between two identical laser beams. One can measure cleave angle by observing the end face and counting the number of interference fringes. Also, the interferometer allows one to observe the general topography of the end face, to see whether it is acceptably smooth or has some imperfection. Of the 90 successive cleaves, only 3 were unacceptable, or 3.3%. It is believed that these were the result of imperfections in the setup.

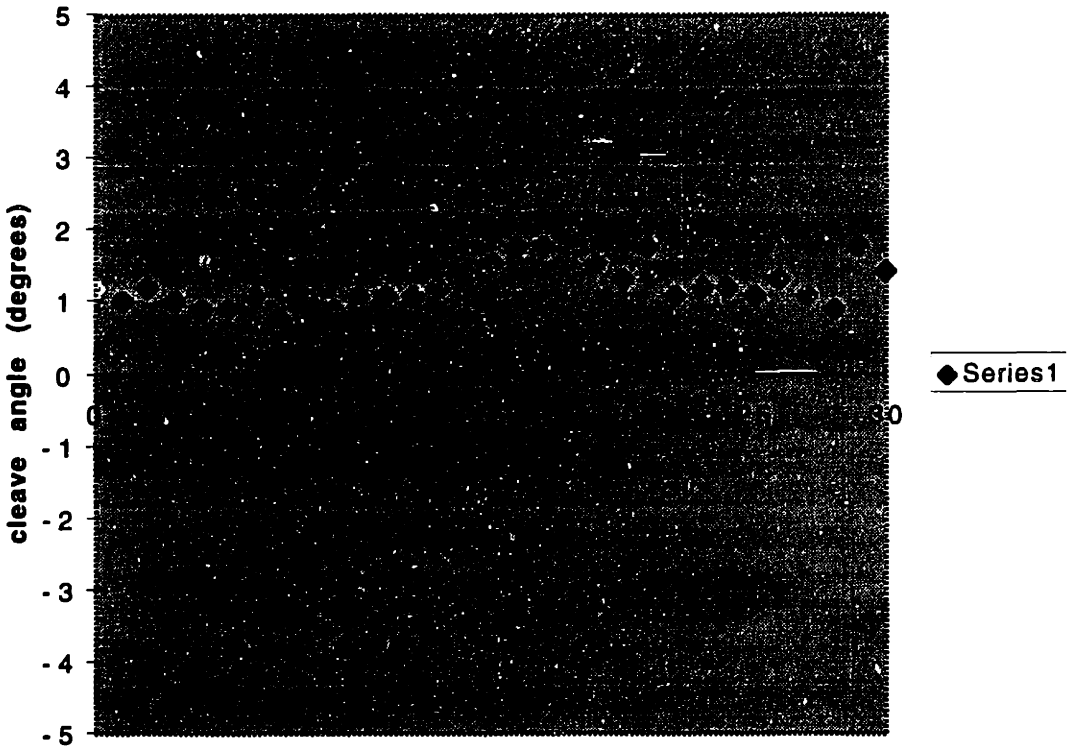

Figure 5.2: PM Cleaving Results

Figure 5.2 shows the results from the 30 continuous PM fiber cleaving runs. The Y axis gives the measured cleave angles while the X axis gives the run number. The average

measured angle for this set of cleaves is 1.25 degrees, and the standard deviation from this average is 0.33 degrees. For this set of runs, all of the cleave angles fell under the 2 degree specification.

5.2 Rejacketing Experiments

The criteria for accepting the Rejacketing Tool is that it be able to perform at least five consecutive rejackets for each fiber size without human intervention or cleanup. These rejackets must be complete and void free, and the fibers must not be damaged by the process.

5.2.1 Experimental Setup

The setup for the testing of the rejacketer consisted simply of the tool itself, and several lengths of center-stripped fiber. Because Fiber Manipulators could not be used for fiber placement, the fibers were guided into the alignment grooves by hand. The piston was then actuated to close the molds. The epoxy was injected using a pressure pump, and the halogen bulbs were powered for twenty seconds. Finally, the molds were open and the sample rejacket was recovered. This process was repeated fifteen times, (five times for each fiber size).

5.2.2 Rejacketing Results

Several problems emanated during the rejacketing experiments. The three most prominent of these involved lengthy dispense times, insufficient mold sealing, and fiber damage upon extraction from the molds. It took an average of about a minute for the pressure pump to fill the mold with the highly viscous epoxy. The rubber seal proved incapable of preventing leakage out of the fiber shaped groove. This resulted in rejacketing material spilling outside of the mold, and the need for cleanup after each rejacket. Finally, this flash also solidified with the rejacket, causing the specimen to adhere to the mold. This

prevented the fiber from being smoothly extracted. A great deal of force was required to extract the fiber, and this often resulted in the breaking of the fiber. It was postulated that a less viscous rejacketing material may solve these problems, as it would require less closing force and dispense time. This could eliminated flash, and allow the rejacketer to function as designed.

5.2.3 Move to Outside Vendor.

Another material was not available at the time, however, and another rejacketing tool had been designed by the same company that provided the Splicing Tool. This design is very similar to MIT's rejacketing tool, with fiber-shaped half grooves closing around the unjacketed fibers. The main differences are that the new tool has both molds made of quartz glass polished optically flat, and these molds seal nearly perfectly when closed together. This company has put several years in research and development of a number of different rejacketing tools, and its design promised to meet all of the functional requirements. In the interest of time, it was decided that the OAS would use the new tool in place of the Rejacketing Tool detailed in this thesis.

5.3 Discussion of Splicing Tool

The fusion splicing tool used on the OAS is a repackaged version of the splice head in a Vytran model #FFS-1000 partially automated fusion splicing system. On this system the splice head uses piezo actuators to finely align prepared fiber ends over a CCD camera in X and Y. The Z and Theta movements are performed with separate fiber holding blocks that are manually moved from station to station on the system. The Fiber Manipulation Module was designed to replace these blocks in the splicing process. Before detailing the experiments performed to ensure the compatibility of the FMM with the Splicing Tool, a more detailed discussion of the operation of this tool is in order.

5.3.1 Operation of the Splicing Tool

The splicing operation envisioned for the OAS is as follows:

1. The Fiber Manipulators move two prepared fiber leads into the Vacuum V-grooves of the splice head. These grooves hold the fiber over a CCD camera mounted in the tool. The camera actually looks at two mirrors that close over the fiber. These mirrors are angled 135 degrees apart to give views of the fiber in both the X and Y directions.

2. The vision system uses the piezo actuators and the MIT Manipulators to coarsely align the fibers in X, Y, and Z, and checks that the cleave angles are not over the two degree specification. Figure 5.3 shows a side view image of prealigned fibers as it appears on the vision system's video monitor.

3. If the fibers to be spliced are PM, then the Manipulators pull both fibers back about 500 μm, and the Splice tool switches to 90 degree mirrors that are used to monitor the fiber end faces. The fibers are then rotated to align their principal axes. The mirrors are again switched, and the fibers are moved back into X-Y viewing positions. Figure 5.4 shows an end view alignment image of a PM fiber as it appears on the vision system's video monitor. Here both fibers are aligned at 90 degrees.

4. At this point, the fibers are finely aligned in X and Y. In order to achieve the .1 μm fine alignment, the Manipulators must move the fibers to within 10 μm of each other.

5. The fusing element is moved over the fiber ends and turned on. After a delay of 0.5 seconds (to allow for the fibers to melt) the manipulators perform a "hot push" to join the fibers. The resolution of this push is critical, as missing by as little as 1 μm can result in a poor splice. Figure 5.5 shows a side view image of properly spliced fibers.

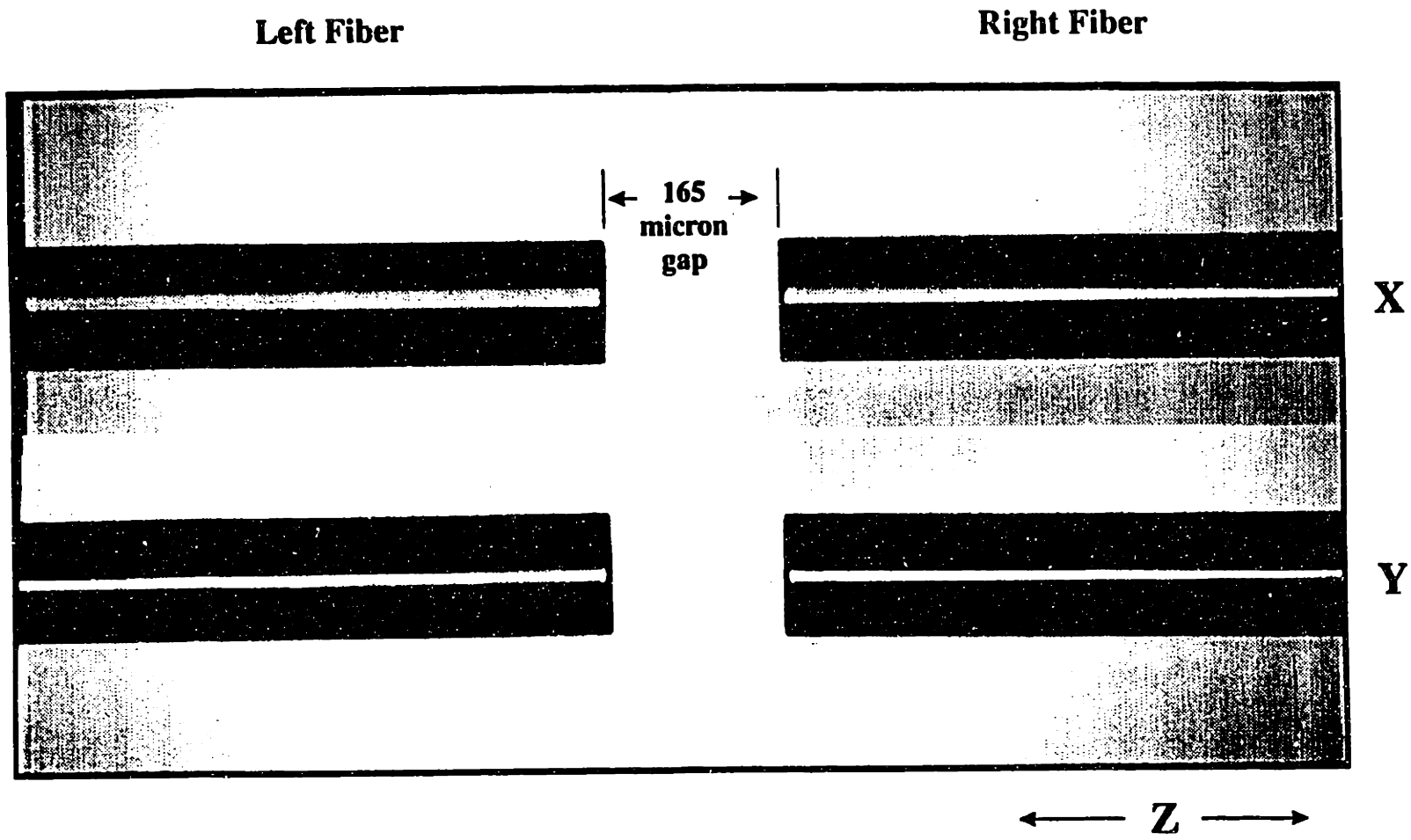

Figure 5.3: Side View Image of Prealigned Fibers

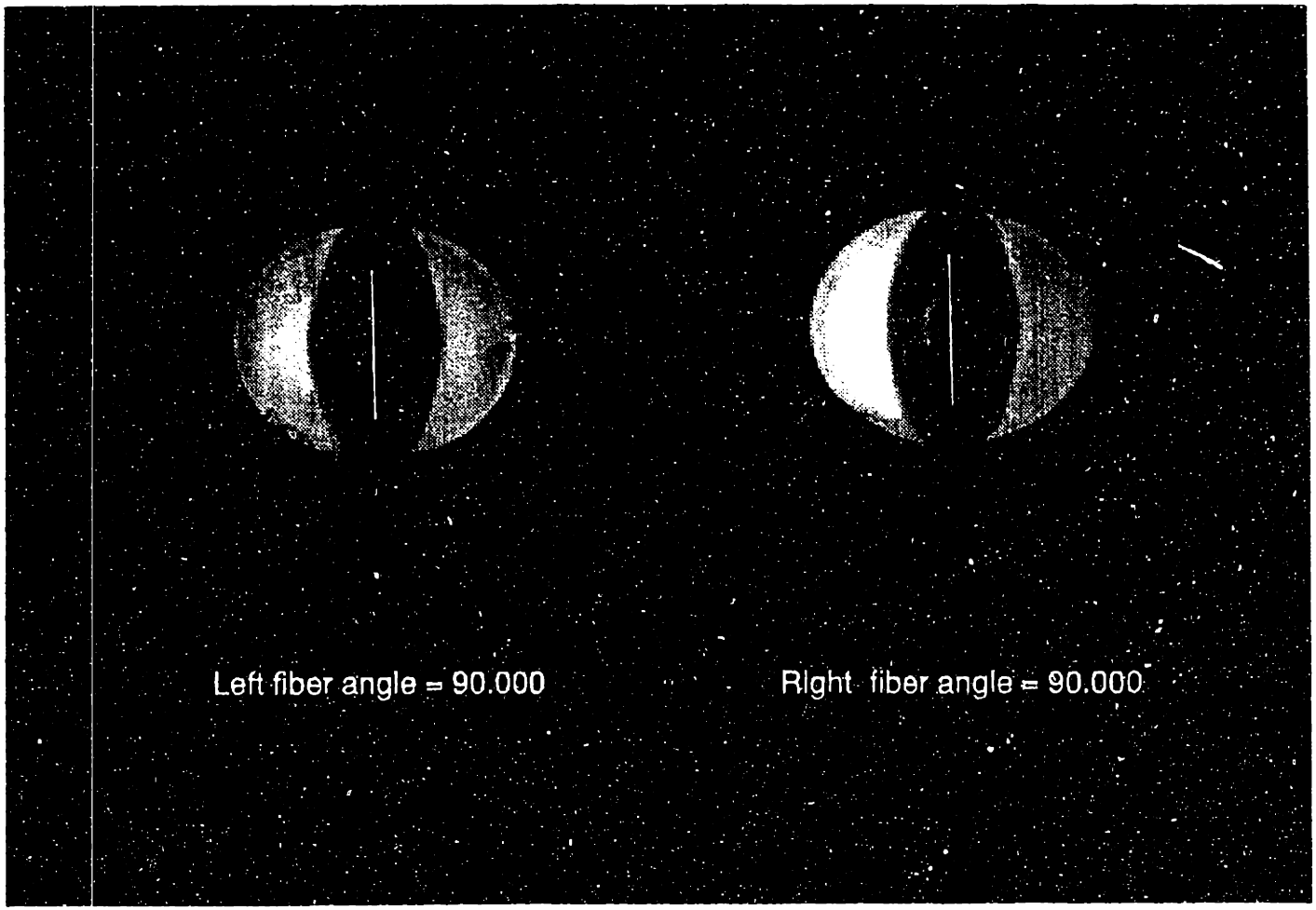

Figure 5.4: End View Alignment Image of PM Fiber

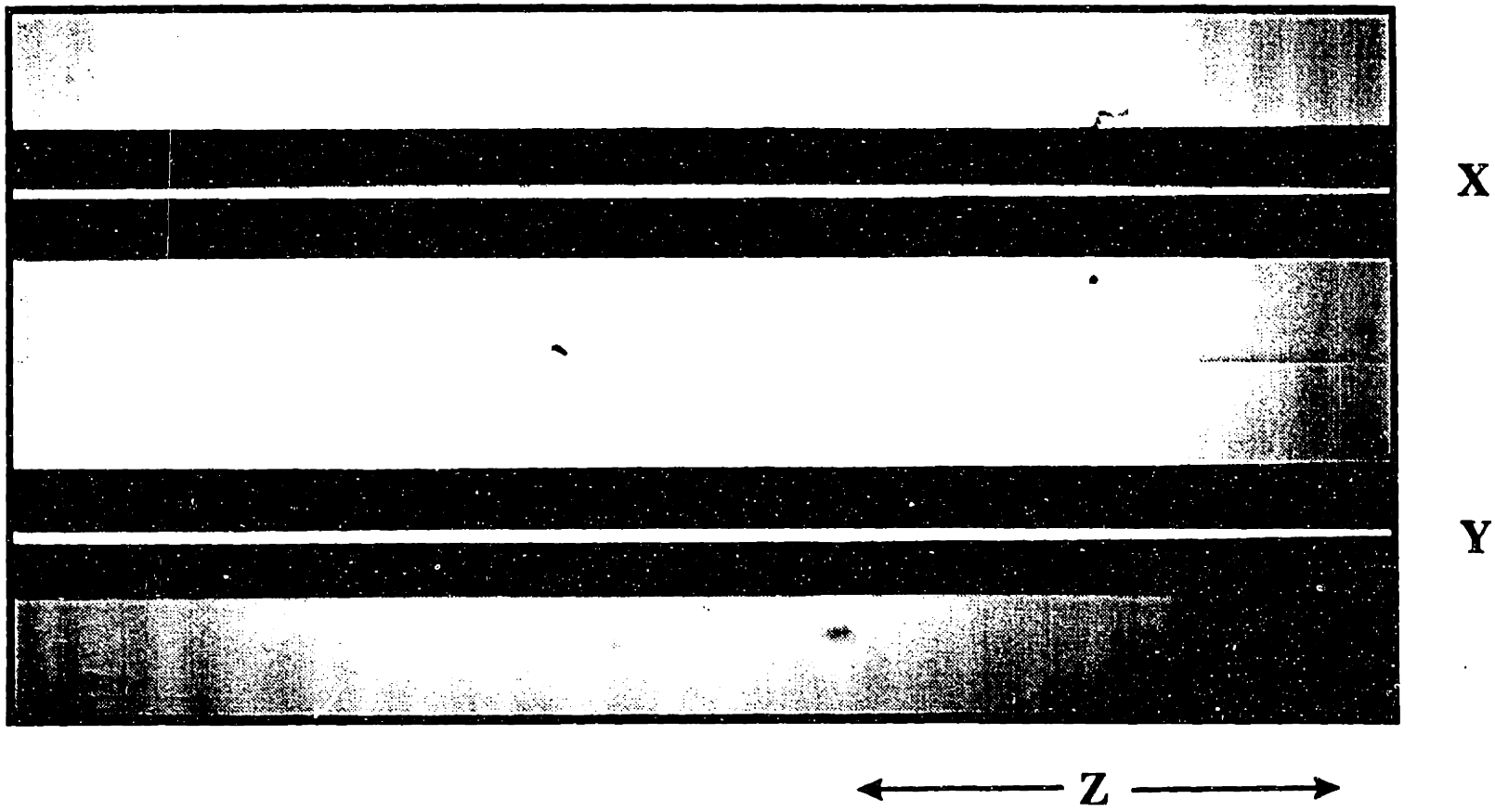

Figure 5.5: Sideview Image of Spliced Fibers

5.4 Splicing Tool Experiments

In order to ensure that the Fiber Manipulation Module could adequately replace the Vytran Fiber holders to perform Z and THETA movements, two tests had to be performed using MIT Manipulators and a Vytran Splicing Tool. The first test consisted of using the manipulators to perform the Z movements in a SM splice. The second consisted of using the Vytran vision system to measure the rotation capabilities of the Manipulators.

5.4.1 Splicing Experiment

Figure 5.4 shows the experimental setup used to perform a SM splice with the Z movements of the Manipulators. It consists of a pair of Manipulators mounted above a Vytran FFS-1000 Fusion splicer. The fiber holding blocks have been removed to allow for the Manipulators. With this setup, the manipulators moved two prepared fiber leads into the vacuum grooves of the fusion splice tool. The vision system and piezo actuators of the tool then worked together to align the fibers in X and Y. The Z stage of the Manipulators performed necessary alignments in theta direction and then moved the fibers as necessary for the hot push. The splice prooftested to 150 kpsi, although no optical power loss was measured. Also, the Vytran vision system was used to ensure that the resolution of the Manipulator Z stage is indeed 0.2 μm.

Figure 5.4: Experimental Splicing Setup

5.4.2 Rotation Experiments

The experimental setup for the rotation experiments was identical to that of the splicing experiments. Here a PM fiber was held stationary in X, Y, and Z, while its elliptical end-face was monitored by the Vytran vision system. This system can calculate the angle of the major axis of the PM fiber's elliptical core. Using these angle calculations, commands were given to the manipulators to rotate the fiber in 45 degree increments from 0 to 180 degrees.

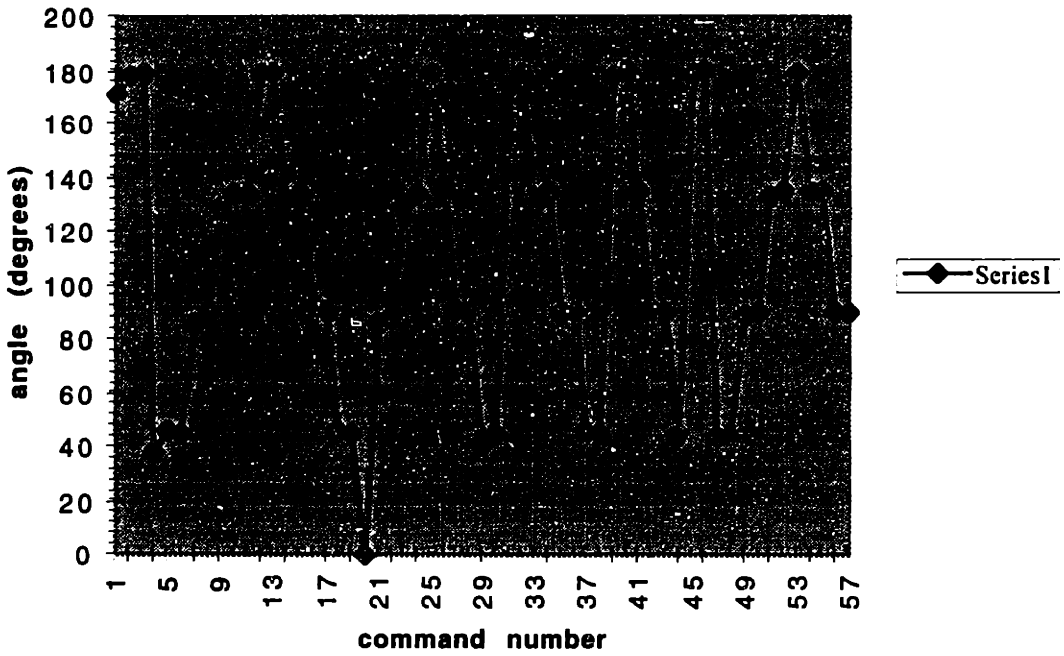

Figure 5.7: Rotation Results

Figure 5.7 shows the results of the rotational resolution experiment. The Y axis represents the target angle given the manipulators, while each data point represents a specific command. It took an average of less than three commands per angle to rotate the fiber to a given angle within the specified +/- 0.5 degrees of error. Also, these experiments confirmed that the resolution of the Manipulators is greater than that of the vision system, as during fraction of a degree movements, the vision system would detect no movements even though there was perceptible movement on the video monitor. These experiments made it clear that the Manipulators could adequately replace the Vytran Fiber Holding Blocks.

Chapter 6

6. Machine Testing and Process Optimization

This chapter begins with the integration of the individual modules onto the OAS frame. It then details the testing performed, and breaks down the automated process times. The latest data for process times is then given, followed by recommendations for future work.

6.1 Machine Build

After all components were acquired, they were assembled on to a steel frame. Figure 6.1 shows a picture of the completed Optical Assembly Station.

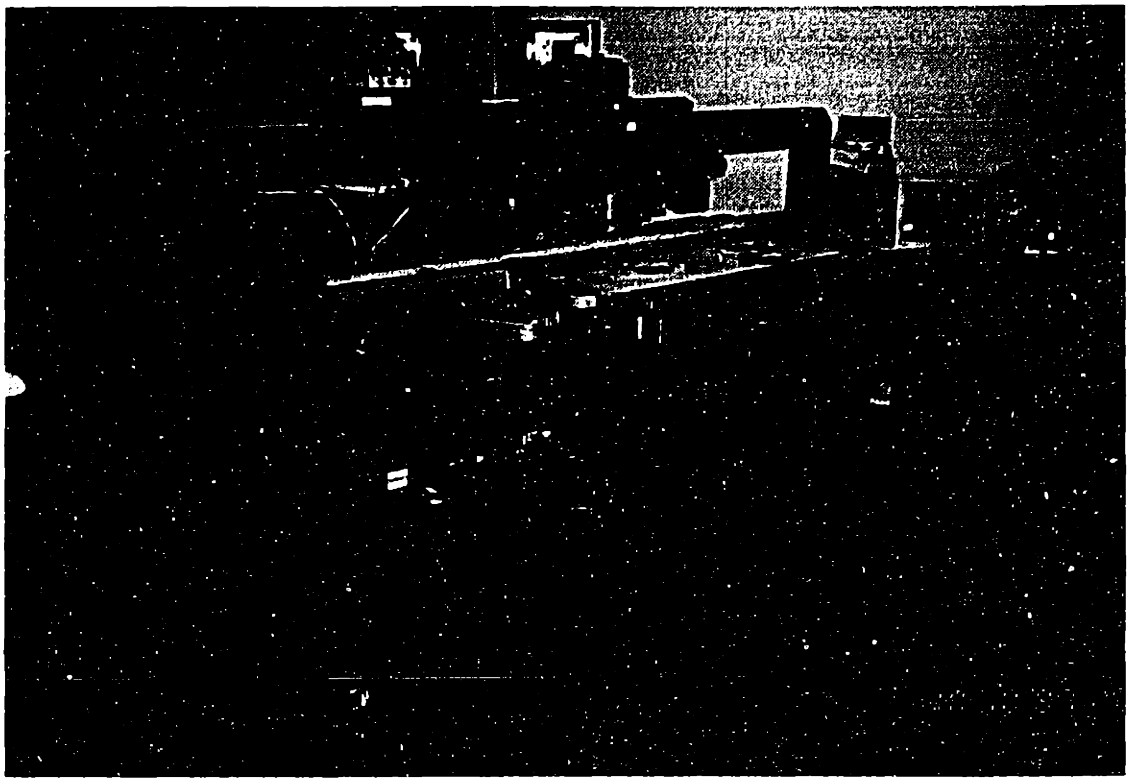

Figure 6.1: Optical Assembly Station

6.2 Machine Testing

After the OAS was assembled, each I/O tested, and each servo and stepper axis tuned, work began on the fiber preparation and splicing processes. A number of issues arose during this phase of development. Each of these issues is discussed below.

6.2.1 Fiber curl

As discussed earlier, the phenomenon called fiber curl, or jacket memory, occurs when a length of fiber has been wound into a small radius for enough time for its acrylate jacket to creep into a curled shape. The OAS process was designed around the idea of maneuvering relatively straight fiber leads. At the onset of testing, it became apparent that many of the fiber leads, particularly PM leads, would exhibit a substantial amount of curl. Depending on the extent of this curl, it could be impossible for the manipulators to even acquire the fiber. Even if they did, problems would appear later as the fiber ends curled away from the grooves and grippers of the various Toolbox items. It was determined that there are two ways to combat this problem. The first is simply to apply heat to the fiber leads once they are loaded on the tray. This tends to equilibrate the residual stresses in the jacket, and straighten the fiber out. The second, and more practical way, is simply to have the operator, or individual loading the components on the tray, arrange the fiber leads such that they curl directly down in Y out of the fiber holding blocks. It was found that if the curl is down, the locators of the Manipulators have no problems acquiring the fiber. Further, the other tools have much less trouble with Y offsets than X.

6.2.2 Laser Power Fluctuations

The fiber leads are stripped by a laser. Specifically, a shield tool on the Tool Changing Module raises underneath the fiber lead, and the laser's marking head moves the beam in a rectangular pattern (back and forth in X while incrementing across the fiber in Z). The speed and power settings for this stripping pattern vary with the type of fiber being

stripped, and once set, any variation from them can result in either a poor strip (if the power is to low or the speed to high), or a damaged fiber, (if the power is too high or the speed to low). It was discovered that for the relatively low powers used on the small fibers, substantial fluctuations in power output could occur. As acquiring a new laser was out of the question, it was decided that the laser itself had to be calibrated on a regular basis.

Another issue that arose with the laser / marking head setup was that after laying dormant for a time (say, overnight) it would fail to activate the laser until the marking head was well into its first strip pattern. This resulted in a good deal of jacket left on the fiber, and was detrimental to further processes down line. It is believed that this behavior is again the result of the low power settings used, as the laser needs to run for a while to clear any startup transients. The solution therefore was simply to make a dummy stripping pattern that operates at the beginning of any OAS startup, before a tray is loaded. It was found that this dummy pattern allowed the laser to reach a steady state and be ready for further processes.

6.2.3 Cleave Tension

As discussed in Chapter 3, proper tension is vital to the cleaving process. During the testing of the OAS, it was observed that at times the fiber would slip in the cleaver grippers, resulting in poor tension and a bad cleave. It was initially thought that this was due to inadequate closing force, and larger pistons were added to the cleaver. When this did not completely solve the problem, it was postulated that the grippers were simply closing too quickly on the fiber, and shattering its jacket and or cladding. The solution was simply to better regulate the flow of air into the piston, (specifically, moving the flow regulators as close as possible to its ports, minimizing the capacitive effects of the air hose.

This allowed the grippers to gently close on the fibers, and hold them repeatably to the specified tensions.

6.2.4 Fiber Splicing

The splicing and rotation tests detailed in Chapter 5 demonstrated that the MIT Manipulators could replace Vytran's fiber holding blocks in the splicing process. The components used in these tests, although essentially identical in design, are not those on the actual OAS. For this reason, effort was required to make the Fiber Manipulation Module compatible with the Splicing Tool. An issue was thought to be the resolution of the Z stage on one of the Manipulators. As previously discussed, the Z movements during a splice are critical. It was discovered that for small moves, one of the manipulators was not always moving the fiber the amount prescribed. Specifically, it tended to move the fiber less than commanded. This resulted in what is called a neckdown, where the fibers are not pushed together enough to blend well together. Such a neckdown is illustrated in Figure 6.1. When a neckdown occurs, the splice is often optically poor and always structurally poor. The solution to this problem emanated from the observation that the Z movements were a function of the position of the lead screw on the stage. It was found that the linear stage was simply not pre-loaded properly, and eccentricities in the lead screw were causing small fluctuations in Z position. Once the proper load was applied to the linear bearings, the splices from the OAS began to fall well within the specifications, as did the resolution of the Z stage.

6.2.5 Incorporation of Safety Features

It was discovered that interference among modules on the OAS presented potentially detrimental situations. After the build, and during the initial testing, it was quite possible to inadvertently cause certain parts of the OAS to come into contact with other parts, resulting in damage to the components. The most common of these was the running of the Tool

Changing Module while a tool was inserted through a tray hole. This caused the tool to hit and drag the tray until it was stopped, either by the user or another critical component. To remedy this situation, software stops were put into the code that prevented certain modules from moving until checks were made. (For the scenario described above, a safety feature was added that prevents the TCM from moving unless all of the Tools are in their home position).

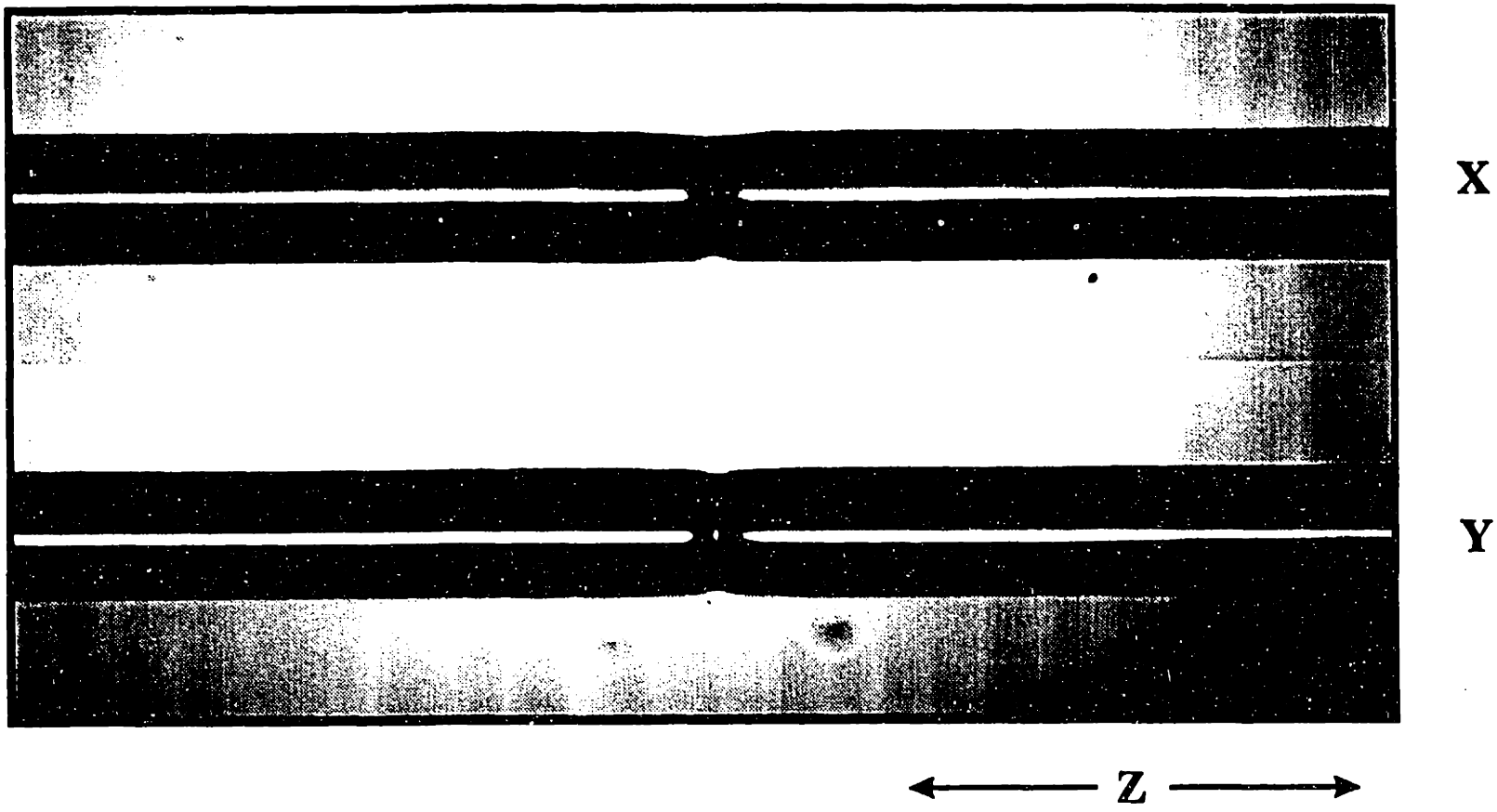

Figure 6.1: Neckdown

6.2.6 Process Time Optimization

At the onset of the testing of the OAS, most of the axes were run very slowly. As well, many pauses and stops were added to the process to allow for safe and observable operation. As the process evolved, the motors were gradually sped up, and the pauses shortened. This time optimization, while not complete, resulted in the automated process times discussed in the following sections.

6.3 Breakdown of Automated Process Times

This section discusses how well the OAS meets the specified process times discussed in Chapter 1. Recall that the current manual process requires about one hour to strip, clean and cleave the fiber ends at a given splice location and to splice, rejacket and prooftest any one point in a circuit. Also, the splice to splice movement in the current process takes 4 minutes. The target times for the OAS is 6 minutes for fiber preparation (stripping, cleaning, and cleaving), 6 minutes for splicing, Rejacketing, and prooftesting, and a splice to splice movement of 0.5 minutes.

Recall the conceptual OAS process detailed in Chapter 2. The following list revisits these steps , but in doing so breaks them down into overall module procedures (Roberts p. 101):

1. Component tray is loaded onto workstation.
2. Component tray is maneuvered so that tray hole #2 is in the fiber work location.
3. Photodetector is docked at tray hole #2,
4. Component tray is maneuvered so that tray hole #2 is in the fiber work location.
5. Right fiber lead is prepared (stripped, cleaned, and cleaved).
6. Left fiber lead is prepared (stripped, cleaned, and cleaved).
7. Opposing Fiber leads are aligned and spliced.

8. Splice is rejacketed and prooftested.

9. Component tray is maneuvered so that tray hole #2 is in the fiber work location.

10. Photodetector is retrieved from tray hole #2.

11. Steps 2-10 are repeated for the next tray hole, etc.

In order to better understand the time breakdown of the OAS process, it is useful to categorize the above steps into four categories. These are the fiber preparation category, the fiber splice category, splice to splice movement category, and the photodetector movement category. Each of the above steps (except the loading of the tray, which only occurs once a circuit) fits within one of these categories. The above list can now be restated with the appropriate category next to each step.

1. Component tray is loaded onto workstation.

2. Component tray is maneuvered so that tray hole #2 is in the fiber work location. [SPLICE TO SPLICE MOVEMENT]

3. Photodetector is docked at tray hole #2. [PMM MOVEMENT]

4. Component tray is maneuvered so that tray hole #2 is in the fiber work location. [SPLICE TO SPLICE MOVEMENT]

5. Right fiber lead is prepared (stripped, cleaned, and cleaved). [FIBER PREP.]

6. Left fiber lead is prepared (stripped, cleaned, and cleaved). [FIBER PREP.]

7. Opposing Fiber leads are aligned and spliced. [FIBER SPLICE]

8. Splice is rejacketed and prooftested. [FIBER SPLICE]

9. Component tray is maneuvered so that tray hole #2 is in the fiber work location. [SPLICE TO SPLICE MOVEMENT]

10. Photodetector is retrieved from tray hole #2. [PMM MOVEMENT]

11. Steps 2-10 are repeated for the next tray hole, etc.

Using this revised list, the process times can now be broken down into concrete areas to improve.

6.4 Process Data

Several weeks of process optimization resulted in the following process time breakdown:

1. Component tray is loaded onto workstation. 60 sec
2. Component tray is maneuvered so that tray hole #2 is in the fiber work location. 8 sec
3. Photodetector is docked at tray hole #2. 30 sec
4. Component tray is maneuvered so that tray hole #2 is in the fiber work location. 8 sec
5. Right fiber lead is prepared (stripped, cleaned, and cleaved). 180 sec
6. Left fiber lead is prepared (stripped, cleaned, and cleaved). 180 sec
7. Opposing Fiber leads are aligned and spliced. 180 sec
8. Splice is rejacketed and prooftested. 180 sec
9. Component tray is maneuvered so that tray hole #2 is in the fiber work location. 8 sec
10. Photodetector is retrieved from tray hole #2. 30 sec

It can be seen from the above breakdown that the entire time necessary for one splice is 874 seconds, or 14.6 minutes. This number, although greater than the 12.5 minute specification, is a dramatic improvement over the current manual process time, and steps are currently being taken by the sponsor to decrease it further.

6.5 Conclusions and Recommendations

This thesis has presented the design and testing of major components of an automated Optical Assembly Station, specifically the design of a Fiber Cleaving Tool, a Rejacketing Tool, and the integration of a Fusion Splicer. The OAS is currently being used to complete IFOG circuits at a company, where work is continuing in the area of automated process time optimization.

One recommendation for the further cycle time reduction of the OAS is to further speed up the servo axes. The speeds that they are currently operating at are by no means optimal. It is believed that by doing this that at least another 3 minutes could be taken off the process. Another recommendation is to redesign the cleaning tool. This tool currently requires the manual application of acetone. A new design that automatically performs this application would greatly reduce the human labor involved in the process. It has also been postulated that, once the process has become repeatable enough, it may no longer be necessary to measure power loss at each splice. More process testing, however, is necessary to validate this postulate. Photodetector movements would then be limited to before and after each circuit. Implementation of these recommendations would reduce the cycle time to well within the specifications.

References

Draper, C.S., "Gyroscope," *Colliers Encyclopedia 1996*, Volume 11, pp. 560-563.

Eberhard, D., Voges, E., "Fiber Gyroscope With Phase Modulated Single-Sideband Detection," *Optics Letters*, Vol. 9(1), 1984, p. 22.

Ezekiel, Shaoul, "An Overveiw of Passive Optical 'Gyros'," in *Physics of Optical Ring Gyros*, SPIE Vol. 487, p. 13, 1984.

Lefevre, H.C., "Evolution of the Fiber Optic Gyroscope," in *Springer Proceedings in Physics: Optical Fiber Sensors*, Vol. 44, p. 124, 1989.

Hentschel, C., *Fiber Optics Handbook: An Introduction and Reference Guide to Fiber Optic Tchnology and Measurement Techniques*, 2nd Edition, Hewlett Packard, Federal Republic of Germany, 1988.

Hsiao, Wen Kai. Master's Thesis from the MIT department of Mechanical Engineering, 1998.

Klass, Philip, "Fiber Optic Gyros Now Challenging Laser Gyros," in *Aviation Week & Space Technology*, July 1, p.62,,1996.

Pavlath, G.A., "Fiber Optic Gyro Development at Litton," in *Fiber Optic Gyros 10 th Anniversery Conference*, SPIE Vol. 719, p. 24, 1986.

Roberts, David. Master's Thesis from the MIT Department of Mechanical Engineering, 1997.